DEVELOPMENT OF DECISION SUPPORT METHODS FOR RESTORATION IN EARTHQUAKE-DAMAGED MEDIUM VOLTAGE ELECTRICITY DISTRIBUTION NETWORKS

DEPREMDEN ZARAR GÖREN ORTA GERİLİM ELEKTRİK DAĞITIM ŞEBEKELERİNDE RESTORASYON İÇİN KARAR DESTEK YÖNTEMLERİNİN GELİŞTİRİLMESİ

MERVE BAYRAKTAR

ASST. PROF. DR. BURCU GÜLDÜR ERKAL

Supervisor

Submitted to

Graduate School of Science and Engineering of Hacettepe University

as a Partial Fulfilment to the Requirements

for be Award of the Degree of Master of Science

in Civil Engineering

2021

To My Parents

ABSTRACT

DEVELOPMENT OF DECISION SUPPORT METHODS FOR RESTORATION IN EARTHQUAKE-DAMAGED MEDIUM VOLTAGE ELECTRICITY DISTRIBUTION NETWORKS

Merve BAYRAKTAR

Master of Science, Department of Civil Engineer

Supervisor: Asst. Prof. Dr. Burcu GÜLDÜR ERKAL

May 2021, 67 pages

From past to present, there have been many destructive earthquakes in Turkey, they still do, these earthquakes show that this region is an earthquake region that has been shaken by serious damages and destructions. The 2020 Elazig and Izmir earthquakes have again revealed that this reality has always existed and how much damage it can cause; it is highly probable that the outcome of the Istanbul earthquake, which may take place at the same magnitude, will be much worse. An earthquake cannot be stopped or prevented, but the material and moral damage it causes can be minimized thanks to the preparations that can be made previously. Current estimations indicate that if another major earthquake occurs, significant damage will occur in earthquake-prone areas. One of the biggest problems that prevent the management of the post-earthquake process, which increases

the loss of life after the earthquake, is the power cuts. Today, electricity has become the main source for the continuation of life and its constant presence in human life has thrown its importance in many areas out of focus, but the power cuts experienced in post-disaster situations have revealed that electricity can stop the activity of many things that work directly or indirectly today. Although transportation and communication are the biggest and main situations that it affects, the fact that it affects the operability of hospitals after the earthquake seriously triggers the loss of life. Therefore, after the earthquake, it is necessary to re-electrify as soon as possible. The focus of this study is to provide input data that can be used in the Markov Decision Process (MDP) based decision support system developed for re-electrification. Being able to accurately determine the post-earthquake condition of the electrical distribution systems is one of the basics for the correct operation of this system; in this study, a series of fragility analyses were performed to obtain the probability of damage to the electrical distribution systems. The main focus of the study is the buildings with electricity distribution systems in the basement in Istanbul, Kadıköy - Güzelyalı district. These electrical distribution systems not only supply electricity to the building under which they are located, but also distribute electricity to the surrounding buildings. After an earthquake that severely damages these buildings, said electrical distribution systems may become unusable and cannot distribute electricity to their surroundings. Some of these electricity distribution systems are located in locations critical to the entire electrical distribution system of the region, and severe damage to these stations can cause disruptions in the distribution system. To investigate this situation, possible damage to 6 specific buildings and their underlying electrical distribution systems was examined. As part of developing the decision support framework for the restoration of the medium voltage electricity distribution network damaged by the earthquake, detailed analyses of these buildings were carried out for the most critical locations in the said region. The buildings were modeled on real floor plans using the SAP2000 program, and nonlinear time history analysis was performed for 60 real earthquake records in each building. The analysis results obtained from the examined buildings were used to create a fragility curve for various damage situations. These fragility curves were then used as input for the Markov Decision Process (MDP) based decision support system developed to rapidly re-electrify the regional electricity distribution system.

Keywords: Fragility Curve, Post-Earthquake Reconnaissance, Nonlinear Time History Analysis, Re-electricity

ÖZET

DEPREMDE HASAR OLUŞAN ORTA GERİLİM ELEKTRİK DAĞITIM AĞLARINDA RESTORASYON İÇİN KARAR DESTEK YÖNTEMLERİNİN GELİŞTİRİLMESİ

Merve Bayraktar

Yüksek Lisans, İnşaat Mühendisliği Bölümü

Tez Danışmanı: Asst. Prof. Dr. Burcu GÜLDÜR ERKAL

Mayıs 2021, 67 sayfa

Geçmişten günümüze Türkiye'de çok sayıda yıkıcı deprem oldu, hala olmaya devam ediyor, bu depremler gösteriyor ki bu bölge ciddi zararlarla ve yıkımlarla sarsılan bir deprem bölgesidir 2020 Elazığ ve İzmir depremleri bu gerçeğin hep var olduğunu ve ne kadar büyük ölçüde zararlar verebileceğini tekrar gözler önüne serdi; aynı büyüklüklerde gerçekleşebilecek İstanbul depreminde ortaya çıkacak sonucun çok daha kötü olması kuvvetle muhtemeldir. Deprem durdurulabilir veya önlenebilir bir durum değildir ancak öncesinde yapılabilecek hazırlıklar sayesinde verdiği maddi ve manevi zarar en aza indirilebilir. Mevcut tahminler, başka bir büyük depremin meydana gelmesi durumunda, depreme yatkın bölgelerde önemli hasar görüleceğini göstermektedir. Depremden sonra can kaybını arttıran deprem sonrası sürecin yönetilmesine engel olan en büyük

sorunlardan bir tanesi yaşanan elektrik kesintileridir. Günümüzde elektrik; hayatın sürdürülebilmesi için temel kaynak haline gelmiştir ve insan hayatındaki sürekli varlığı çoğu alandaki önemini arka plana atmıştır ancak afet sonrası durumlarda yaşanan elektrik kesintileri elektriğin günümüzde doğrudan ve dolaylı olarak çalışan pek çok şeyin faaliyetini durdurabileceğini gözler önüne sermiştir. Ulaşım ve iletişim etkilediği en büyük ve temel durumlar olmasına rağmen deprem sonrasında hastanelerin çalışabilirliğini de etkiliyor olması can kaybını ciddi oranda tetiklemektedir. Dolayısıyla depremden sonra yeniden elektriklenmenin en kısa sürede sağlanması gerekmektedir. Bu çalışmanın odak noktası, yeniden elektriklenme için geliştirilen Markov Karar Süreci (MKS) temelli karar destek sisteminde kullanılabilecek girdi verileri sağlamaktır. Elektrik dağıtım sistemlerinin deprem sonrası durumunu doğru tespit edebilmek bu sistemin doğru çalışabilmesi için temellerinden birisidir, bu çalışmada elektrik dağıtım sistemlerinin hasar görebilme olasılıklarını elde edebilmek için bir dizi kırılganlık analizleri yapıldı. Çalışmanın asıl odak noktası İstanbul'un Kadıköy-Güzelyalı bölgesinde yer alan bodrum katında elektrik dağıtım sistemleri bulunan yapılardır. Bu elektrik dağıtım sistemleri sadece altında bulunduğu binaya elektrik sağlamakla kalmaz aynı zamanda çevredeki binalara da elektrik dağıtır. Bu binalara ciddi hasar veren bir deprem sonrasında, söz konusu elektrik dağıtım sistemleri kullanılamaz hale gelebilir ve çevresine de elektrik dağıtamaz. Bu elektrik dağıtım sistemlerinden bazıları bölgenin tüm elektrik dağıtım sistemi için kritik olan konumlara yerleştirilmiştir ve bu istasyonların ciddi şekilde hasar görmesi dağıtım sisteminde kesintilere neden olabilir. Bu durumu araştırmak için, belirli 6 bina ve onun altındaki elektrik dağıtım sistemlerinde olası hasar incelendi. Depremde hasar görmüş orta gerilim elektrik dağıtım şebekesi restorasyonu için karar destek çerçevesi geliştirmenin bir parçası olarak bu binalarda ayrıntılı analizler, söz konusu bölgedeki en kritik konumlar için gerçekleştirildi. Binalar, gerçek kat planları üzerinden SAP2000 programı kullanılarak modellendi ve her binada 60 gerçek deprem kaydı için doğrusal olmayan zaman alanı analizi yapıldı. İncelenen binalardan elde edilen analiz sonuçları, çeşitli hasar durumları için bir kırılganlık eğrisi oluşturmak için kullanıldı. Bu kırılganlık eğrileri daha sonra bölgesel elektrik dağıtım sistemini hızla yeniden elektriklendirmek için geliştirilen Markov Karar Süreci (MDP) tabanlı karar destek sistemi için girdi olarak kullanıldı.

Anahtar kelimeler: Kırılganlık eğrisi, Elektrik Dağıtım Sistemleri, Markov Karar Sistemi, Deprem Sonrası Keşif

ACKNOWLEDGMENT

First of all, I have to express my gratitude to Asst. Prof. Dr. Burcu GÜLDÜR ERKAL, my supervisor, for the patient guidance, valuable advice, criticism, encouragement and understanding during my thesis study Ever since I started working with her, she has been both a guide and a mentor for me at every step that needs to be completed and every stair that needs to be climbed.

I want to to thank Assoc. Prof. Dr. M. Abdullah SANDIKKAYA and Assoc. Prof. Dr. Alper ALDEMİR for sharing their valuable knowledge with me in the fields of ground motion, and 3D modeling in SAP2000 computer program.

Also, I have to give thanks to Assoc. Prof. Dr. Baki ÖZTÜRK, Asst. Prof. Dr. Burcu GÜLDÜR ERKAL, Assoc. Prof. Dr. M. Abdullah SANDIKKAYA, Assoc. Prof. Dr. Alper ALDEMİR and Asst. Prof. Dr. Ebru GÖL for giving me the opportunity to defend my master thesis.

This study was supported by The Scientific Research and Technical Council of Turkey (TUBİTAK), Project No: 118E183.

Thanks for due to the support of our study Kadıköy municipality sharing with us the floor plans of Kadıköy and EnerjiSA sharing the transformer panels.

Finally, I would like to express my deepest appreciation to my family who always stand behind me and never lose their support and understanding throughout my whole life.

TABLE OF CONTENTS

LIST OF FIGURES

LIST OF TABLES

SYMBOLS AND ABBREVIATIONS

Symbols

$F_{\_}(x)$	Fragility Function
M_w	Magnitude
R_{JB}	Joyner-Boore Distance
S_a	Spectral Acceleration
S_{ae}	Spectral Acceleration
S_s	Short Period Spectral Acceleration Coefficient
S_1	Spectral Acceleration Coefficient for A 1.0 Second Period
Vs_{30}	Average Shear-Wave Velocity
x	Particular Value for Roof Displacement
$Z_{1.0}$	Shear-Wave Velocity of 1.0 km⁄s
μ	Mean
σ	Standard Deviation
Φ(s)	Standard Normal Cumulative Distribution Function

Abbreviations

APEC	Asia-Pacific Economic Cooperation Energy Working Group
CDF	Cumulative Distribution Function
CS	Conditional Spectrum
FBPF	Forward-Backward Sweep Power Flow
GMPM	Ground Motion Prediction Model
PEER	Pacific Earthquake Engineering Research Center
PGA	Peak Ground Acceleration
PMDP	Markov Decision Process
PSHA	Probabilistic seismic hazard analysis
RSN	Record Sequence Number

SAP	Structural Analysis Program
DER	Distributed Energy Resources

1. INTRODUCTION

1.1 General

The security of energy supply is a major concern, given the strong dependence on the society functioning for adequate distribution. The smooth functioning of modern society is entirely at the basis of electrical energy in today's world, such that many basic services (water, gas, communication, etc.) are provided depending on the continuity of electricity, which brings the continuity of electricity to a vital point

It is of great importance that re-electrification is carried out as soon as possible in order not to interrupt the communication infrastructure, which is the prerequisite for the rapid delivery of aid teams and vehicles to the earthquake regions after a possible earthquake. Possible power cuts that occur after the earthquake pose a threat not only for communication, but also for the supply of drinking water, the sustainability of treatment plants and the continuation of the services of hospitals.

1.2 Literature Review

The effect of natural disasters on electricity distribution systems concerns countries all over the world, especially those in the earthquake region. Electrical supply is one of the most critical and at the same time the least reliable services after the earthquake. There may be hospitals that could not provide services despite the lack of structural damage as a result of the lack of continuity of electricity after the earthquake; for example, after the 1999 Kocaeli earthquake, half of the hospitals could not be supplied with electricity [1]. Figure 1 shows the photographs of the damaged buildings after the 1999 Kocaeli earthquake [2]. These photos show that it is not possible to predict whether the electricity distribution systems in the basements will be able to operate after the earthquake without calculating how much damaged each building can be. It is very clearly seen in Figure 1 that the electrical distribution systems of the buildings in (a) and (b) cannot work; in (c) and (d), there is a possibility that the systems are working.

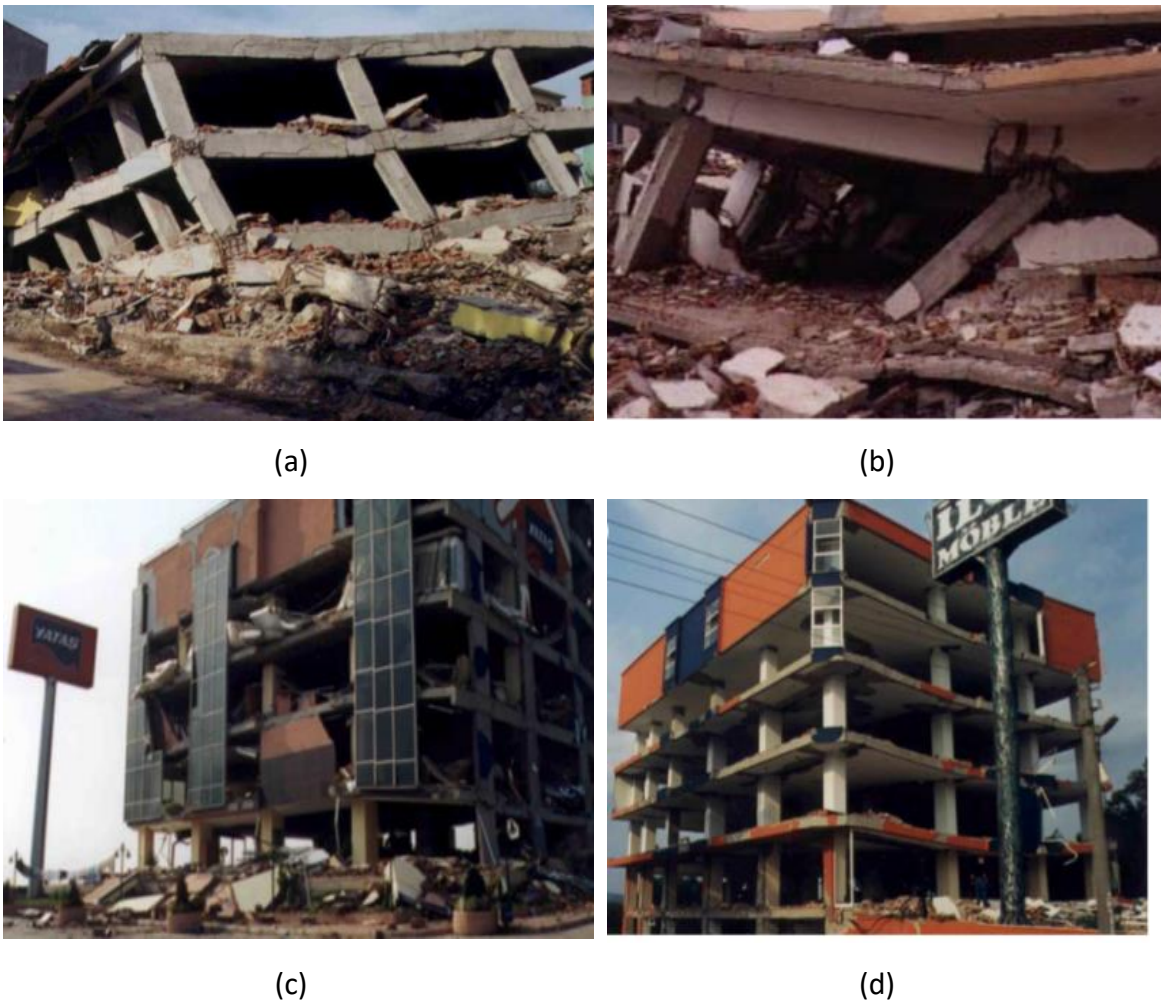

Figure 1 Photographs of buildings damaged after the 1999 Kocaeli earthquake [2]

These power cuts after the earthquakes occurred in Kobe, Japan in 1995, and the entire earthquake region remained without power for a period of three to five days according to the report reporting the damage [3]. In Northridge, USA, the same power cut occurred for one day in 1994; a few moderate earthquakes caused power cuts, either blocking power flow to the entire network or significantly damaging a single station. In a study conducted by M. Shinozuka et al., a seismic system performance analysis was performed on the electrical power system of the Los Angeles Department of Water and Power, providing inventory data, system configuration, and fragility information with or without rehabilitation [3]. M. Shinozuka et al. conducted system deterioration analysis by calculating the average power output ratio associated with the system under nondestructive conditions for each service area. In the system analysis, a Monte Carlo simulation method was used under the hypothetical fragility curves shown in Figure 2(a). Figure 2 shows this system and its fragility curves.

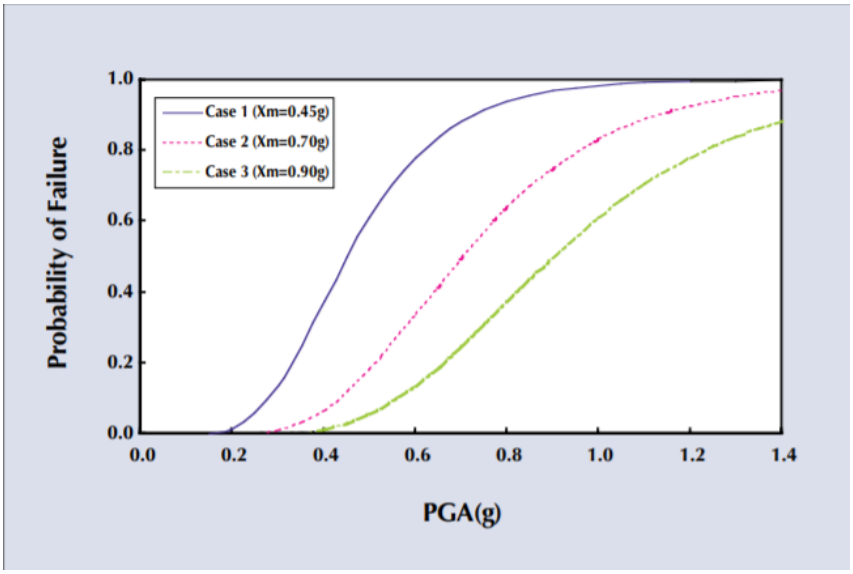

(a)

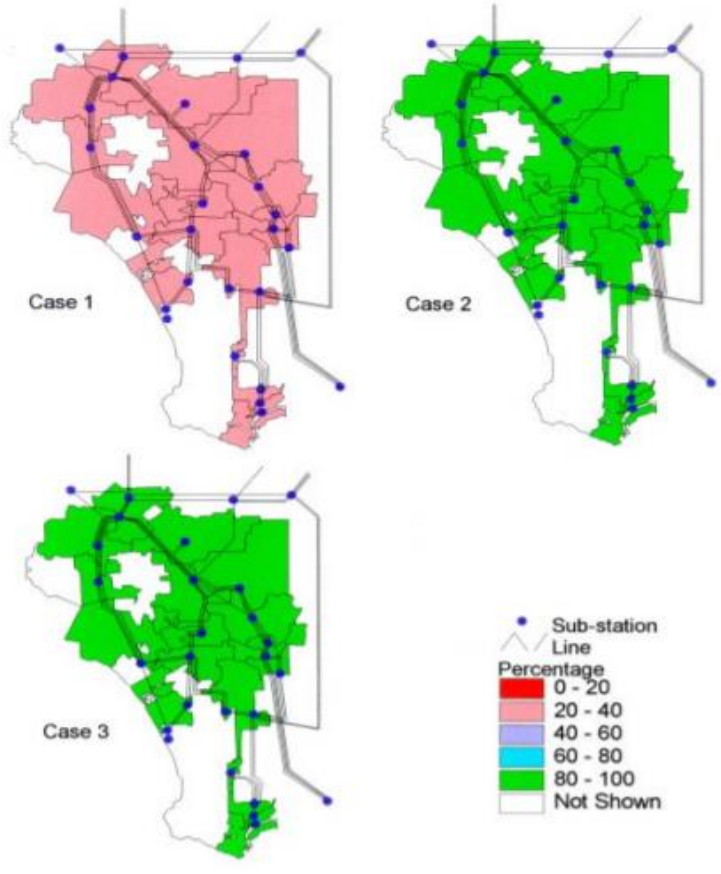

(b)

Figure 2 (a) Fragility Curves Relative and (b) Average Power Output (revisited from M. Shinozuka et al., 1999 [3])

All these studies show that post-earthquake disaster management studies focusing on electrical energy supply, energy supply systems, response plans, earthquake risk assessment and management is developing worldwide and progress has been made in different areas, for example seismic performance analysis of electrical power systems have been the main subject emphasized in the studies of Energy Working Group [4] , M. Shinozuka et al. 2007 [5] and M. Shinozuka et al. 2003 [6]. In APEC economies, the energy supply system is always under the risk of earthquakes. Since earthquakes are unpredictable, it is challenging for APEC economies to ensure that energy supply systems remain secure even during a major earthquake.

APEC clarified the cuts in electrical systems and their consequences after the Manzanillo earthquake [4]. In this earthquake, the loss of 345 kV on 28 transmission lines caused the Chiamin and Lungchi Substations to be disconnected from the grid, resulting in the interruption of power transmission from South to North. All of Central and Northern Taiwan was immediately blacked out. Table 1 shows the number of damaged transmission lines [4].

Table 1 Number of Damaged Transmission Lines (APEC, 2002)

	Transmission Towers						
Lines	Collapsed	Titled	Deformed	Foundations cracked or subsided	Foundations displaced	Total	No. of Lines Damaged
345 kV	1	9	55	271	19	355	28
161 kV	9	4	9	157	4	197	30
69 kV	3	16	3	60	2	84	21

Regarding the transmission network of electrical power systems, M. Shinozuka et al. described sequential failures of the receiving station components under a severe earthquake in 2007 study [5]. They assumed that circuit breakers and disconnect switches were restored more rapidly with uniform probability density during the first 12-hour period and with transformers and buses during the first 24-hour period. This reflected not only indirectly the relative ease of repairing/replacing each component, but also the cost of replacement. Figure 3 shows the restoration probability function.

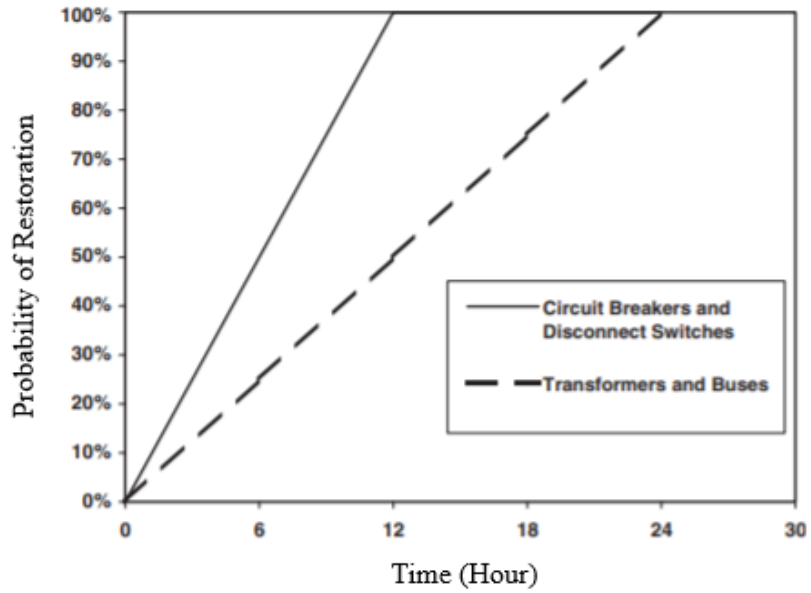

Figure 3 Restoration curve for transformers, circuit breakers and disconnect switches [5]

M Shinozuka et al. 2003 [6] evaluated the performance of electrical power systems before and after a major catastrophic event such as accidental or man-made failure of system components, such as an earthquake; accordingly, retrofitting was carried out for 69 and 161 kV systems; the effectiveness of these studies is shown in Figure 4 [6].

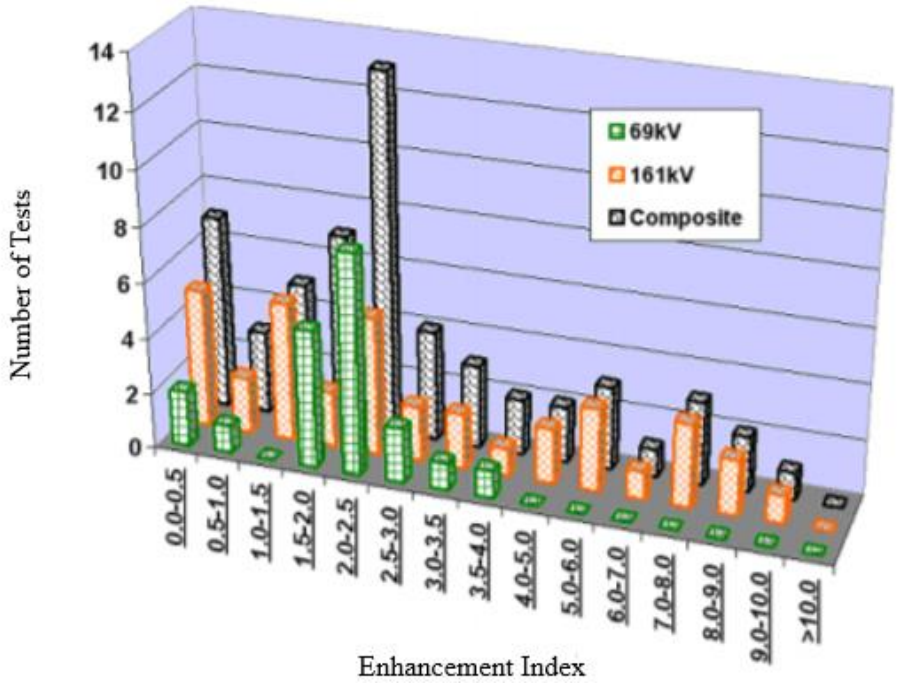

Figure 4 Statistical Distribution of Enhancement of Transformers

Another example for seismic performance analysis of electric power system in power installation design criteria for dealing with investigated earthquakes was carried out by G. Parise et al. [7]. For these seismic performance analyses, a study was carried out on modeling the fragility of system components described by N. C. Rasulo et al. [8].

T Adachi et al. [9] explained the effect of damage to the supporting electrical power system using a fault tree analysis and a shortest path algorithm, and in this study, the uncertainty of seismic intensity was evaluated by the effect of component fragility on network integrity.

I. Chevalier et al. 2006 [10] made a strong warning about Europe's dependence on imported energy, which could rise from 50 percent in 2000 to 70 percent in 2020-2030. Because energy supply security is a recurring concept in national energy policies and also at the European and world level. M. Shinozuka et al. [11] developed an analysis procedure and a database to evaluate the performance of electrical power and water supply systems before and after a major catastrophic event such as an earthquake, accidental or man-made failure of system components. K.Y. Spencer et al. 2008 [12] developed an approach to predict the seismic performance of complex critical urban infrastructures and to optimize the seismic retrofit of infrastructure systems based on system-level performance under the constraint of limited resources.

The effect of these systems on generation, transmission and distribution infrastructure after the earthquake was investigated by J.E. Araneda et al. [13].

A framework for analyzing the vulnerability of independent infrastructure systems has been developed by S. Wang et al. [14]. At the beginning of the studies on the activity of post-earthquake electrical systems, Z. Cagnan et al. [15] describes the post-earthquake restoration process for electrical power systems. In addition, M. Ouyang et al. [16] used a probabilistic modeling approach to measure the hurricane resistance of contemporary electrical power.

The restoration of electrical grids has been the subject of evaluation in many studies from various aspects [18] – [24] F. Qiu et al. 2017 [18] and Z. Zhao et al. 2018 [19] suggested network restoration methods for possible disasters (pre-disaster) . Where and how strongly an earthquake occurs directly affects the vulnerability of structures. Therefore, an infinite

number of destruction scenarios can occur as a result of an earthquake. This limits the usability of stand-up scenarios developed before a disaster occurs.

In this study, online decision support methods used to re-electrify electricity distribution systems were also discussed by other researchers [21] – [24]. N Ganganath et al. [21] modeled this as a constrained optimization problem and proposed a partitioning strategy to solve it in three steps. In the first step, some available methods and expert knowledge were used to initiate the partitioning process, in the second step the modeled constraints were met, and in the third step, he worked to find suitable partitions for parallel restoration. In the study by LHTF Neto et al. 2016 [22] presented an intelligent method of service restoration for electrical power systems as power system restore is a procedure to restore the power supply after a power outage.

The importance of fast and safe re-electrification after major grid outages has led to the definition of individual power system restoration plans. The risk of power outages increases as systems approach their limits. Therefore, existing restoration strategies and plans for changing conditions should be evaluated. An automated approach has been proposed by M. Ostermann et al. to evaluate strategies and restoration plans for extra-high voltage networks [23]. C. Loh et al. 2001 [24] presented an analytical method for developing fragility curves of highway bridges whose post-earthquake efficiency was greatly affected. Since past earthquakes such as the San Fernando earthquake of 1971, the Northridge earthquake of 1994, the Great Hanshin earthquake of 1995 in Japan, and the Chi-Chi earthquake of 1999 in Taiwan have shown that bridges are vulnerable to earthquakes, and the seismic fragility of road bridges is often expressed in terms of fragility curves.

In these methods and studies developed for the re-electrification process, predictive data in the literature are used according to the scenario that occurs, not directly from the field. However, in this study, data prepared according to the data coming directly from the field and according to the characteristics of the earthquake are used. Since in order for electricity distribution systems to work fully, system observability must be fully ensured. In the absence of observability, it is not possible to use the methods in the literature. Since these methods assume that the network model is known exactly, but this is an assumption that is far from reality. However, the proposed decision support system has been developed to provide support even without observability.

Despite so much work on examining and improving the post-earthquake and post-hurricane situation, this study serves as; An online decision support method could not be developed for the re-electrification of damaged medium voltage electricity distribution networks after the earthquake.

1.3 Objective and Scope

The aim of this study is to develop a field support software that will help re-electrify the medium voltage electricity distribution system as soon as possible after an earthquake occurs. The biggest difference that distinguishes post-earthquake power cuts, which form the center of this problem, from an operational failure is the changes in the network structure due to the earthquake. The main reason for these changes is that some system elements (electric poles, panels, transformers, etc.) are damaged and unusable due to earthquakes.

After an earthquake has occurred, it is essential to recover electrical energy to critical electrical loads such as hospitals, military bases and important government offices. Therefore, re-electrification should be completed as soon as possible. After a major collapse of the electrical grid, the problem of escalation has been studied by researchers for years and given a certain maturity. While re-electrification is a problem in itself, it becomes more difficult to solve in disaster situations. The main reason for this is the collapse of many buildings due to the earthquake and the lack of transportation and communication. Elements of the electrical grid (electric poles, distributed generation facilities, distribution transformers) can be directly damaged during and after an earthquake, as these elements can become unusable by the collapse of surrounding structures.

This study aims to prepare accurate inputs that represent real data in the field for use in a system that will provide decision support to system operators to recover the electrical grid. The decision support system to be developed can use the feedback from the site, as well as detect the possibility of damaging the network elements by using the earthquake data, so the best energizing strategy to follow in this context is the operator.

This study consists of 8 main sections, in the first of these sections, which are the cause and effect of each other, general information about the literature review and the aim of the study is given.

In the second section, the selection procedure of the specific buildings on which the analyses will be carried out in the selected pilot region is explained in order to be able to perform the fragility analysis, which is the main objective of the study.

In the third section, the real floor plans of the buildings selected in the second section using the SAP2000 building analysis program and 3D models made using the building input parameters are explained. In this section, the effect of using real and accurate data on such systems is revealed.

In the fourth section, the process of obtaining real earthquake data, which is one of the main conditions for real and specific fragility curves, is explained.

In the fifth section, nonlinear time history analyses made in the SAP2000 program using the real earthquake records selected in the previous section and the results obtained for these analyses are explained.

In the sixth section, the use of lognormal cumulative distribution function and the fragility curve creation procedure were explained by using the results obtained in the fifth section in the analytical steps that are planned to be followed in order to obtain fragility analysis.

In the seventh section, which is the ultimate aim; The Markov Decision Process (MDP) based decision support system, in which the fragility curves obtained will be used as input, is explained.

In the last part, the fragility curves obtained in this decision support system are used as inputs and the effect of this study on the re-electrification process is shown with real examples.

2. STRUCTURE SELECTION

Power cuts that occur after an earthquake cause different dangers directly and indirectly and constitute a major obstacle to resolving the post-earthquake chaos. These power cuts both prevent communication after the earthquake and can cause fires if re-electrification is not provided. In order to prevent cuts, situations that threaten the safety of electricity distribution systems during and after an earthquake should be identified first. At this point, the vulnerability of the buildings surrounding the system during earthquakes, which seriously threatens the security of these systems, has been the starting point of this study. In this study, the probability of damage to the buildings surrounding these systems was calculated in order not to interrupt the activities of the electricity distribution systems, and the data obtained were used to re-electrify the electricity distribution systems. This study describes all the details of the process of obtaining the fragility curves to be used as input for the MDP-based decision support system developed for the recovery of the electricity distribution system after the earthquake. The fragility curves used for damage estimation in seismic risk assessments are generated for building types with similar characteristics in a particular country or region. Since the creation of fragility curves according to regional characteristics and building floor plans is a difficult and laborious task in general, existing fragility curves created as a result of international studies are used for damage estimations. However, since these simulated fragility curves cannot be suitable for all the details of the buildings and the ground on which the buildings are located, in fact, the conducted works can sometimes diverge from the truth, thus prolonging the post-earthquake re-electrification process. For this reason, in this study, the specific fragility curves obtained by meticulously doing all the necessary studies on the existing structures were used. Since the fragility curves are directly related to the dynamic analysis results of the buildings, the buildings to be modeled should be selected first.

2.1 Electric Distribution Plan

At this point, since the main aim is to examine the effect of possible damage to the buildings on the electricity distribution systems, the building selection to be made can be defined as deciding which buildings will affect the transformers of these systems. Transformers of electrical distribution systems inside or around the building may become unusable due to damage to the buildings in a possible earthquake; Therefore, the electricity distribution plans of the Kadıköy region were obtained from EnerjiSA in the selection of the buildings to be

modeled. Figure 5 shows the distribution plans for the 10 kV single line scheme and the 35 kV single line scheme. In this section, the main electricity providers, the electrical routes coming out of them, the transformers providing electricity on these routes and the addresses of the transformers are shown.

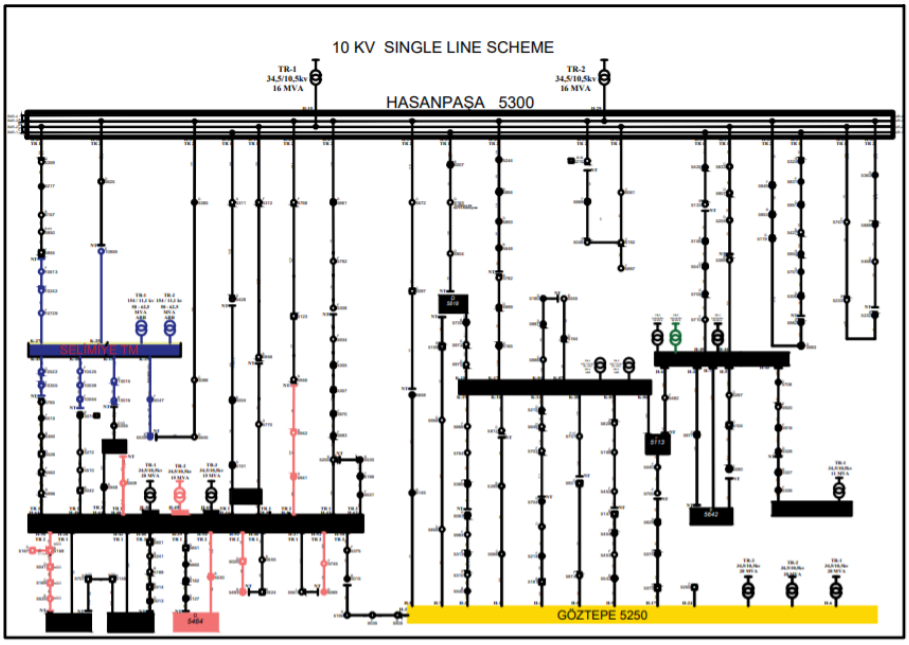

(a)

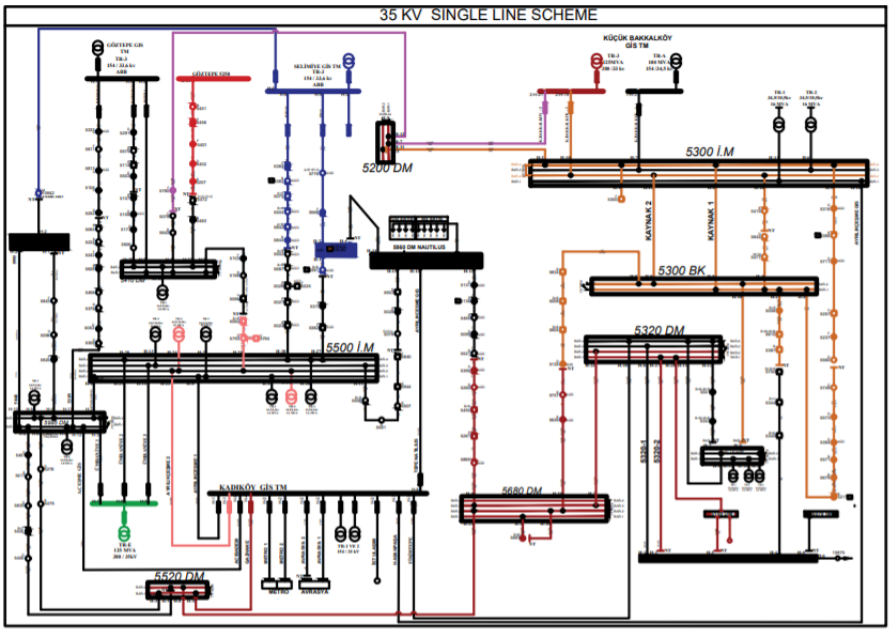

(b)

Figure 5 Electric Distribution Plans (a) 10 kV single line scheme (b) 35 kV single line scheme

On these plans received from EnerjiSA, electricity distribution systems were examined and transformer numbers and addresses were listed. Since most of the listed addresses do not have an address number, that is, the address indicates a region rather than a specific location, and there is no building within a distance that may affect the electricity distribution systems, many locations were excluded from the scope of the study; the remaining locations were determined as buildings with electrical distribution system transformers in or around them. Locations in the list are marked on the map to check the accuracy of existing buildings. Table 2 shows the addresses of transformers in electrical distribution systems.

Table 2 Addresses of Electric Distribution Systems

35 kV SINGLE LINE SCHEME		**10 kV SINGLE LINE SCHEME**	
Number of electric distribution system	**Address**	**Number of electric distribution system**	**Address**
10642	Z.Kamil Hospital	5359	Uhuvet Street Iett Lodging Houses Hasanpaşa
5333	Göztepe Park Metro Construction Site	5217	Pomak Street No: 6 Next to Acıbadem
5811	C. topuzlu Street Haluktoezören Street	5157	Köftüncü Street Atabay Pharmaceuticals Next toofactory
5813	F. Garden Neighborhood Muhtar Street	5950	In Acıbadem Köftüncü Sokak Wishofoundation
5105	Cemil topuzlu Street Dr. Kazım Lakay Street	5020	Bayramyeri Street Şadrıvan Passage
5252	Fenerbahcetounaman Street No: 10	5625	Acıbadem Zeamet Street. No: 20 Opposite
5065	Fenerbahce Army House	5385	Mandra Cadde No: 2 Konak Business Center
5224	Fener Kalamış Street. Behind No: 86	5088	Star Street Corner

5242	Fenerbahçe Neighborhood Knowledgeable Street.	5428	Hasanpaşa Kehkeşan Street. Insidetohe Park
5928	M.N. Selcuk Street Kalamis Hotel Garden	5004	Inofront of Acıbadem Sarayardı Street No: 54
5291	Papatyalı Street No: 6 Cemil topuzlu Street	5151	Acıbadem Street And İnkişaf Street Corner
5575	Cemil topuzlu Street No: 13 Garden	5102	Kadıköy Söğütlüçeşme Mosque Under
5503	F. Garden District Dalyan Range Street	5312	Hasanpaşa Neighborhood
5107	Ahmet Mithat Street Corner Next totohe Park	5966	Kadıköy Municipality Garden
5108	Fenerbahça Neighborhood Egemen Street	5946	Back of Poyroz Street
5173	F. Garden District Ahmet Mithat Efendi Street	5942	Poyraz Street. Sadıkoğlu Business Center
5506	Baghdad Street No: 13 American Hospital.	5308	Next to Kuleli Construction Ziverbey Zühtüpaşa Neighborhood.
5780	Pinar Sokak No: 7 Next to Göztepe	5934	Zühtüpaşa District. K. Poet Kahya Street.
5078	Feneryolu Boztepe Street No: 14	5307	Kızıltoprak, Next totorain Station, Kavuklu Hamdi Street
5643	Gazi Muhtarpaşa Street Oppositetoheofixed Market	5683	Bağdat Street Behindofenerbahçe Stadium
5451	Göztepe Neighborhood Bagdat Street	5655	Neşet Omer Streer Kadıköy Passage
5456	Göztepe Neighborhood Bağdat Street Double Pools Secondary School	5530	Next to Kadıköy Marriage office
5401	Göztepe Neighborhood Hattat Bahatin Street	5186	Söğütlüçeşmetorain Station Under
5402	Göztepe Neighborhood, Cavitpaşa Street	5167	Altıyol Çilek Street Ptt Plant
5207	Goztepe Sumer Street No: 1	5168	Altıyol Çilek Street Under Ptt Plant

5483	Göztepe Neighborhood. Street of Roses	5169	Kuşdili Street Ephesus Bazaar Under
5103	Kızıltoprak Bagdat Street Linden Dead Sea	5525	Alisuavi Street Next totohe Church
5166	Baghdad Street No: 91oflorans Nighingen Hospital	5073	Stationery Street Onur Business Center Next
5066	Recep Peker Street Medicana Hospital	5707	Bahariye Street Courthouse Under
5064	Fenerbahce Stand Under	5148	Bahariye Street And İhsan Ünlüer Street Corner
5114	Kurukahveci Street No:2	5801	Hasırcıbaşı 2. Yol Street.
5794	Fenerbahce Stadium	5188	Dr. Esat Işık Cadde Inofront of Anatolian High School
5384	Eyüp Aksoy Street Behind Hatahane	5514	Dr. Esat Işık Street Saint Josehp High Schoolofashion
5383	H. Pasha Numune Hast Earthquake Clinic	5013	Fashion School Street.
5075	Rıhtım Wastewatertoreatment Plants (İsokaki)	5651	Moda Bostan Street No: 44
5842	Caferağa Sports Hall Six Nailbey Street	5127	Moda Cadde Girls High School
5844	Şifa Hospital Caferağa Neighborhood Nailbey Street	5030	Fashion Street. With Dr. Esat Işık Street. Corner
5502	Bahariye Street Kalfaoğlu Street	5015	Kuşdili Street. Inside Yoğurtçu Park
5687	Next to Kadıköy Güneşlibahçe Street No: 49	5035	Recep Peker Street Next toofb Stadium
5026	Behindtoansaş Kadıköy	5505	Baghdad Street Mobile Gas Station Next
5027	Neşet Ömer Street Insidetohe Ptt	5572	Behindofeneryolu Bağdat Caddesi No: 163
5024	Yoğurtçu Şükrü Street	5159	Faruk Ayanoğlu Street No: 26 Under
5776	Harem Inside Port	5970	Fenerbahce Alageyik Street No: 6

5568	Harem Sahil Oyak Concrete Worksite	5244	Kuyubaşı Sarayönü Street No: 40
5381	Haydarpaşa Chest Surgery Hospital	5061	Against Sarayönü Street No: 6
5025	Tansas Kadıköy Behindtohe Post office	5997	Marmara University Goztepe Camp
5317	Haydarpaşa Vocational High School	5156	Behind of Mandra Street No: 218
5382	Dr. Eyüp Aksoy C. Behiçbey Street Asokakeri Dormitory	5953	Dairy Street And Yıldırım Street Cornerofikirtepe
5930	Inside Haydarpaşa Gataofaculty of Medicine	5119	Ankara Asphalt Dmo Warehouse
5903	Kadıköy Cultural Center Six Dock	5324	Dairy Street Yavuz Streettoechnical Building Construction Site
5076	Rıhtımtoramway Management	5104	Hızırbey Street Clusher No:8
5840	Colonelofaik Sözder Street Hotel Interior	5427	Mandra Street And Doğan Street Cornerofikirtepe
5944	Neşet Ömer Street Behind Migros	5306	Eggcı Abdibey Street Next toofbofacilities
5507	Windmilltoeyyareci Sami Street	5982	Eggci Abdibey Street Bahçem Street
5131	Sarayardı Street And Hakkı Street Corner	5983	Dumlupınar Neighborhood. Y. Abdibey Street. Next totohe Mosque
5390	Hasanpaşa Iett Garageofillingofacilities	5889	Hasanpaşa Mirim Çelebi Streetofinance Lodging
5492	Fikirtepe Dairy Street Mandarins	5147	Cavitpaşa Street No:20
5895	Education District 2. Açıkgöz Street No: 21	5858	Goztepe Hasan Ali Yücel Street No: 34
5834	Dairy Street No: 184 Inofront	5360	Fener Kalamaış Street Oppositetohe
5008	Hızır Bey Cadde Usta Construction	5067	Fenerbahce Marina

5135	Hızırbey Street Lightning Street	5984	F. Kalamış Caddeof Bahçe Cape Marina
5757	Education District Muratpaşa Street Orkide Street Corner	5313	Fenerbahçe Boom Galatasarayofacilities
5341	Y. Abdi Bey Streettoechnical Construction	5310	Kadıköyofb Sports Club Socialofacility
5415	Marmara University Goztepe Camp	5812	Feneryolu Street No: 46
5644	Near Marmara University	5289	Baghdad Street Railway Street Burc Site Inside
5477	Marmara University A.B.C.D. Block	5068	Insideofenerbahçe Ordu House
5610	Peace Street Şua İnş	5703	Yıldıray Street No: 11 Next toofeneryolu
5750	Egg Maker Abdibey Avenue Nuhoğlu	5214	Göktepe Street No: 3 Next toofeneryolu
5316	Dumlupınar Neighborhood Şahika Street	5181	Yazıcıbaşı Street No: 1 Under Buildingofeneryolu
5711	Merdivenköy Neighborhoodtoeacher Harun Reşit	5737	Cemil topuzlu Street İşbank Blocks

In order to ensure the distribution of the buildings to be selected in different g values, the buildings are classified according to their g values. Figure 2 shows the classification map according to the g-values of buildings with electrical distribution systems in and around them. The locations in figure 2 show the locations of transformers in the electrical distribution systems in figure 6.

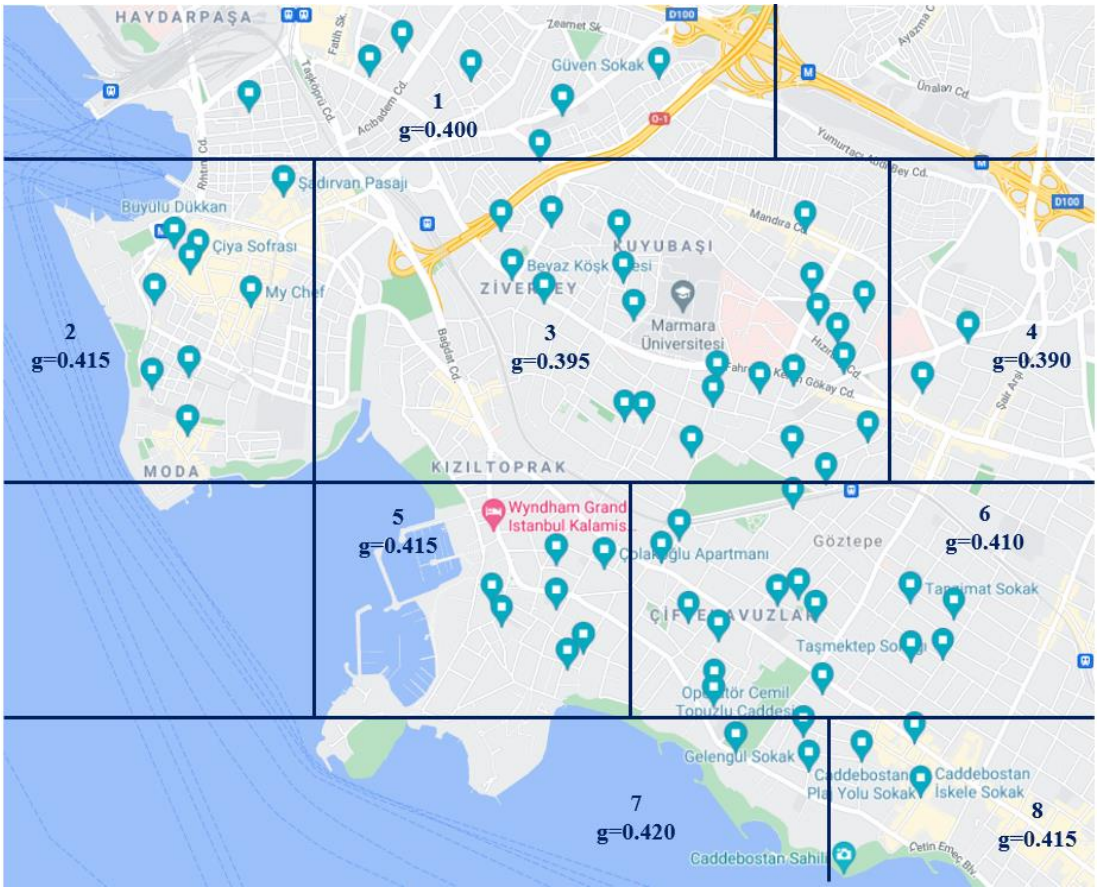

Figure 6 Map of the classification of selected buildings according to g values

2.2. Excursion and Classification of Building

After the classification map was prepared, a trip was organized to Istanbul Kadıköy to check the locations of the buildings with electricity distribution systems in or around them and the transformers around them. During the trip, it was seen that some buildings were demolished, some buildings underwent urban transformation and electricity distribution systems were carried through some buildings. In Figure 7, a few photographs of transformers that were seen in the plans and whose existence was confirmed during the trip are shown.

Figure 7 Photos of electricity distribution systems from excursion

According to the data obtained in this direction, only six buildings were identified within a distance and situation that could damage the electricity distribution systems. The electrical distribution system numbers listed in Table 3 belong to the 6 selected buildings. Figure 8 shows the location of only 6 selected buildings on the map, which previously showed all the locations in the plan. The numbers in the locations correspond to the block and parcel numbers of the buildings. According to the image, since two buildings are in g region 2 and the other buildings are in g region 3,5,6 and 8, g value diversity is provided.

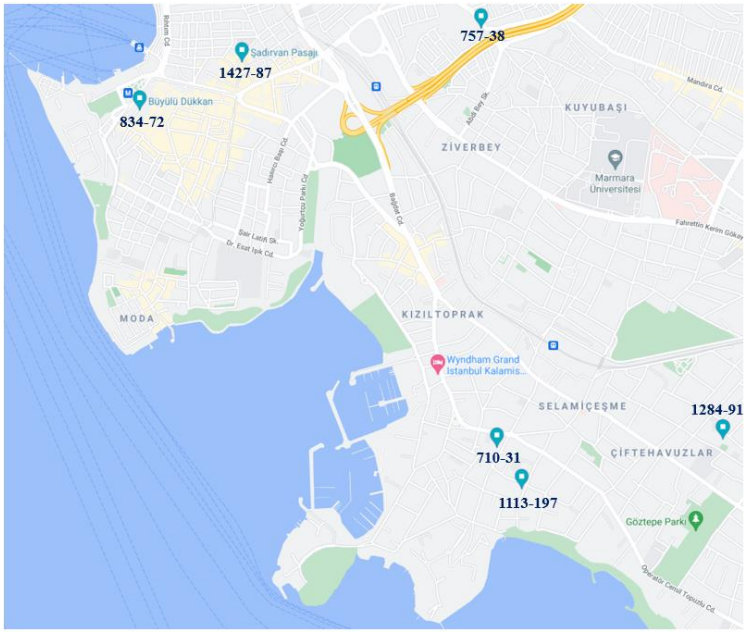

Figure 8 Selected Buildings

The electricity distribution system numbers and full addresses corresponding to the selected buildings are shown in table 3.

Table 3 Electric distribution system numbers for selected buildings

10 kV SINGLE LINE SCHEME		
Number of electric distribution system	Address	Lot and parcel numbers of building
5020	Bayramyeri Street Şadrıvan Passage	1427-87
5655	Neşet Omer Streer Kadıköy Passage	834-72
5159	Faruk Ayanoğlu Street No: 26 Under	710-31
5104	Hızırbey Street Clusher No:8	757-38
5147	Cavitpaşa Street No:20	1284-91
35 kV SINGLE LINE SCHEME		
Number of electric distribution system	Address	Lot and parcel numbers of building
5114	Kurukahveci Street No:2	1113-197

2.3. Floor Plans

Dynamic analysis of the buildings is required in order to create the fragility curves of the selected buildings. In order to do this, the most important required document is the floor plans of the buildings. Since the buildings were built in 1970-1980, Kadıköy Municipality was contacted to get floor plans and floor plans were provided within the scope of the study. Opensees is an open-source program that is planned to be used for analysis before going on a trip. In this program, it is possible to obtain nonlinear time history analysis results that are very close to reality by preparing a 2-dimensional model, however, there are many missing and unreadable parts in the floor plans, since the buildings were built in old years, in this case, it was decided to prepare 3D models using the SAP2000 structural analysis program,

since 2D model drawings can diverge the analysis results from the reality. Figure 9 shows the floor plans provided for each different floor of the buildings.

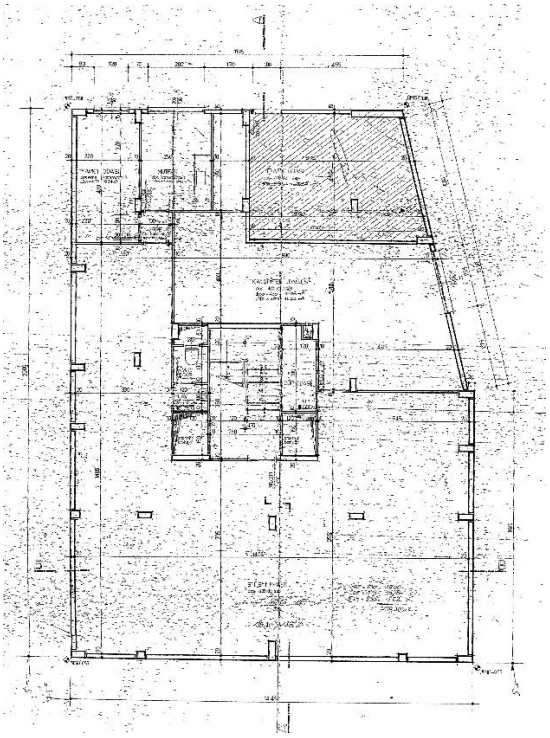

Basement Floor Plan

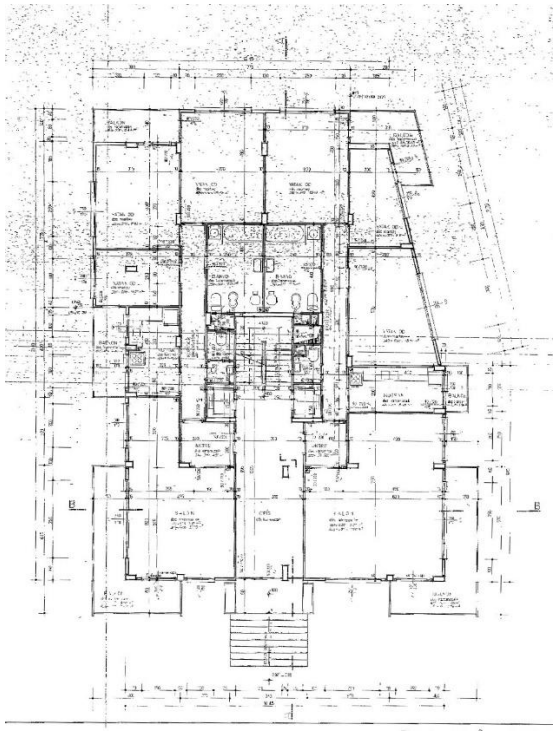

Ground Floor Plan

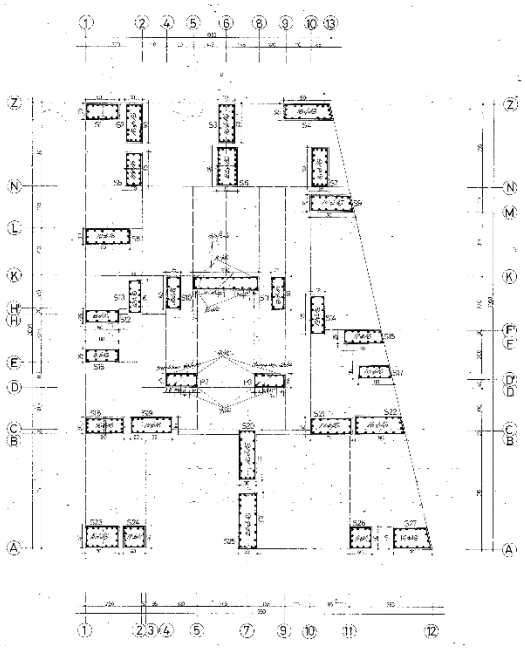

Normal Floor Plan

(a)

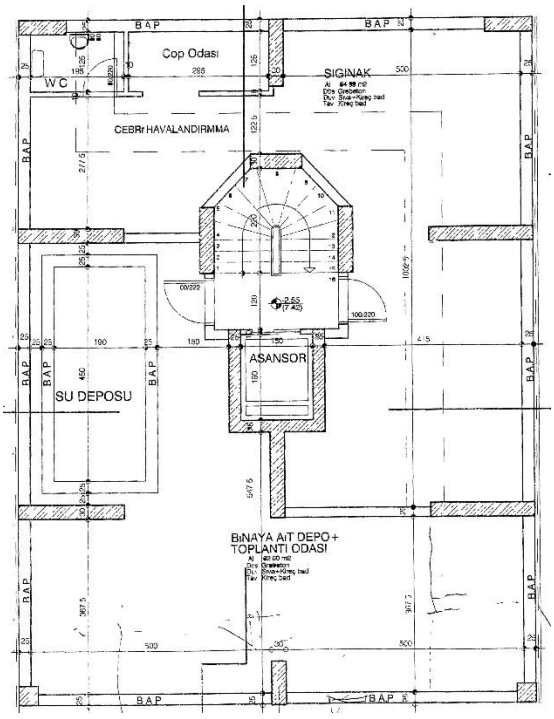

Basement Floor Plan

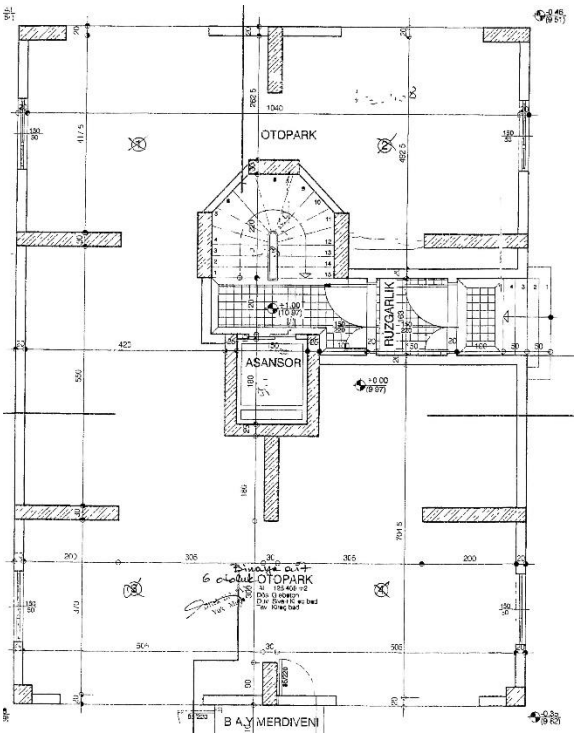

Ground Floor Plan

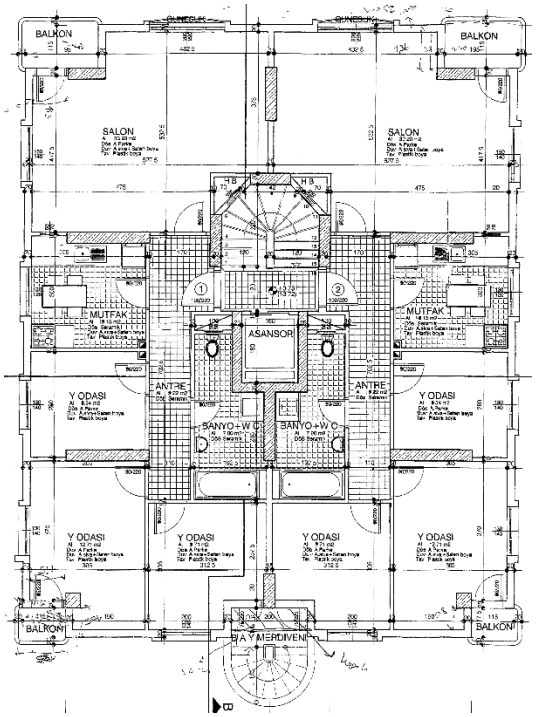

Normal Floor Plan

(b)

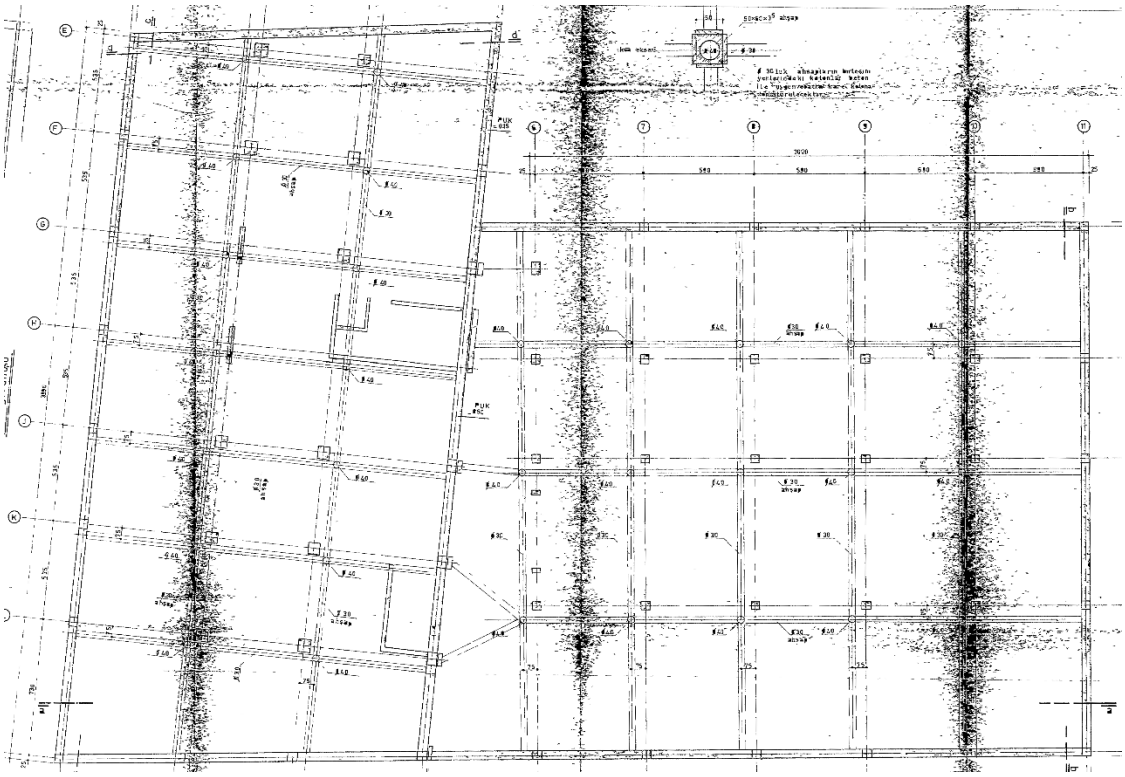

Normal Floor Plan

(c)

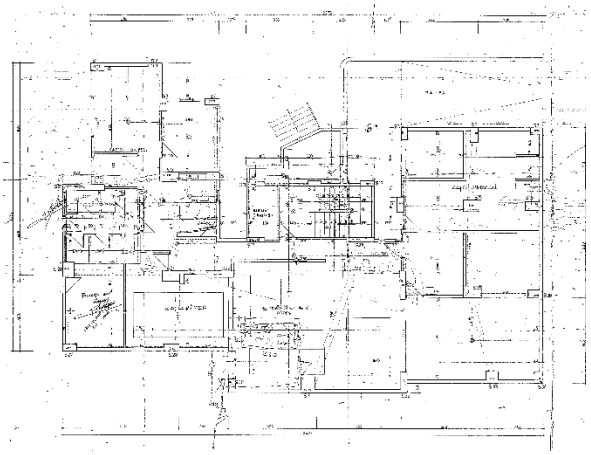

Basement Floor Plan

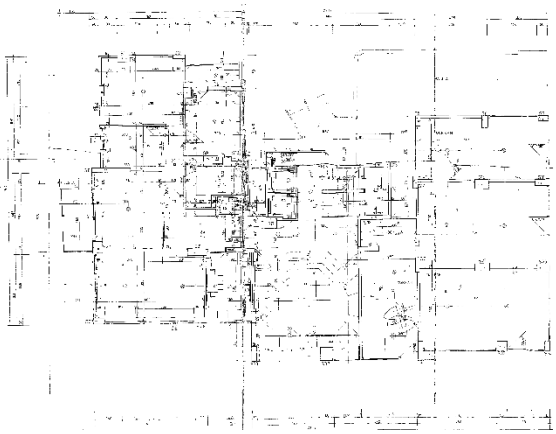

Ground Floor Plan

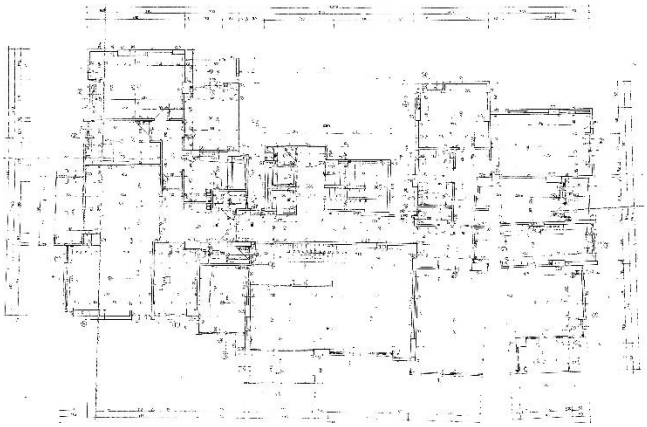

Normal Floor Plan

(d)

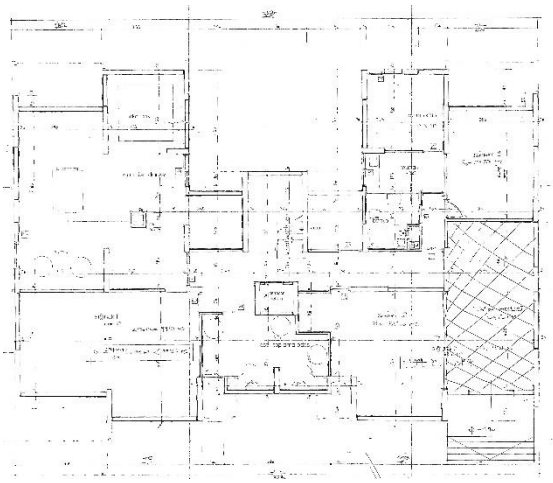

Basement Floor Plan

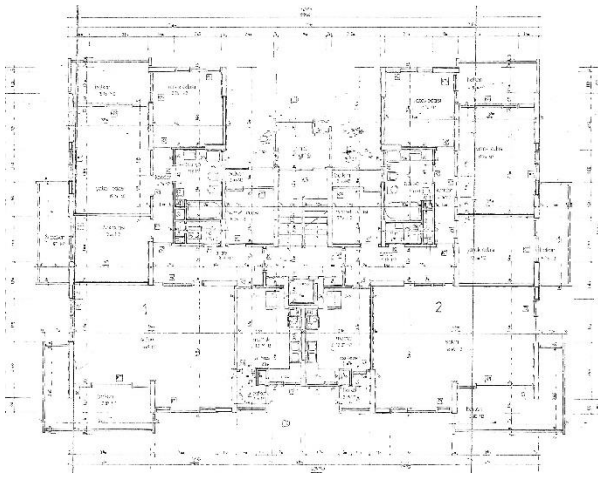

Ground Floor Plan

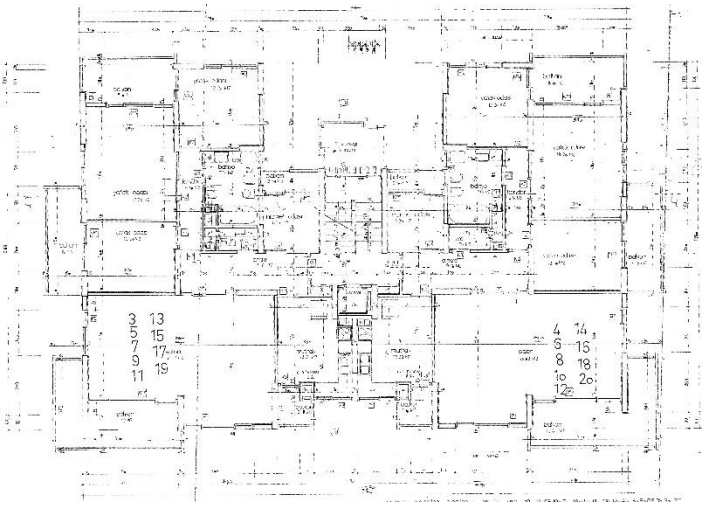

Normal Floor Plan

(e)

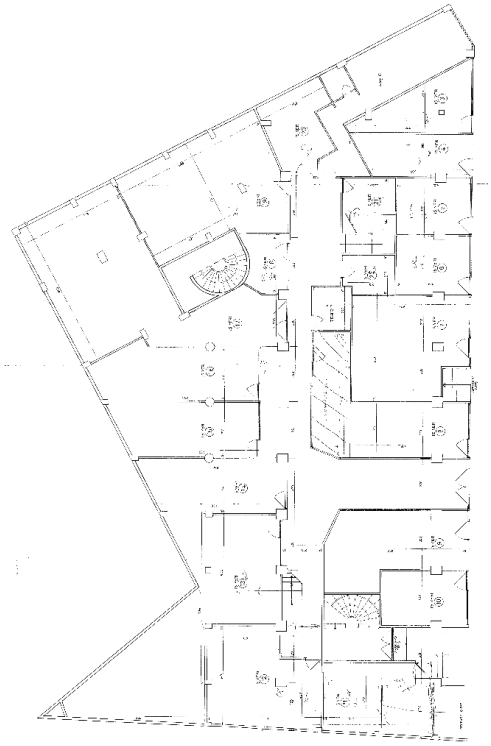

Basement 1 Floor Plan

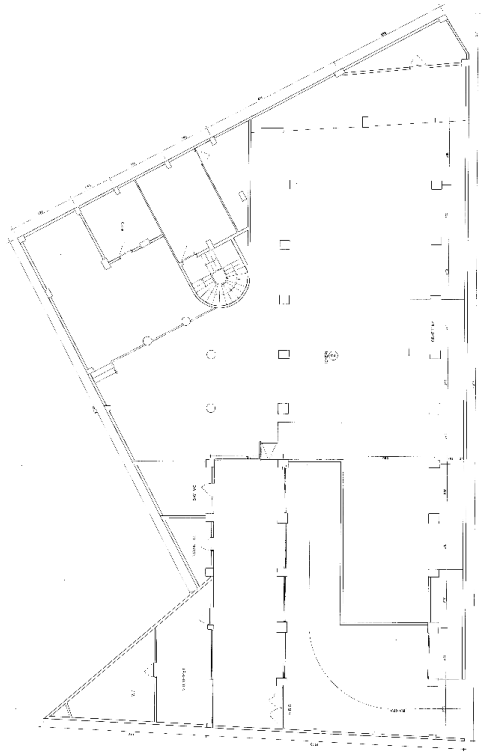

Basement 2 Floor Plan

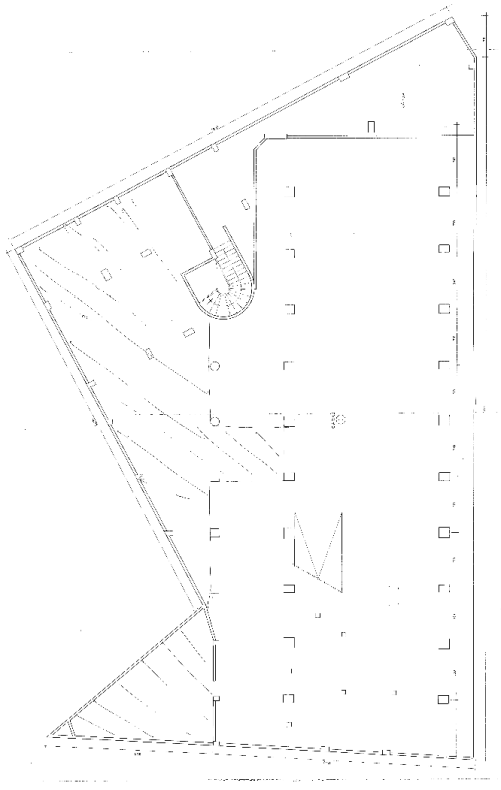

Basement 3 Floor Plan

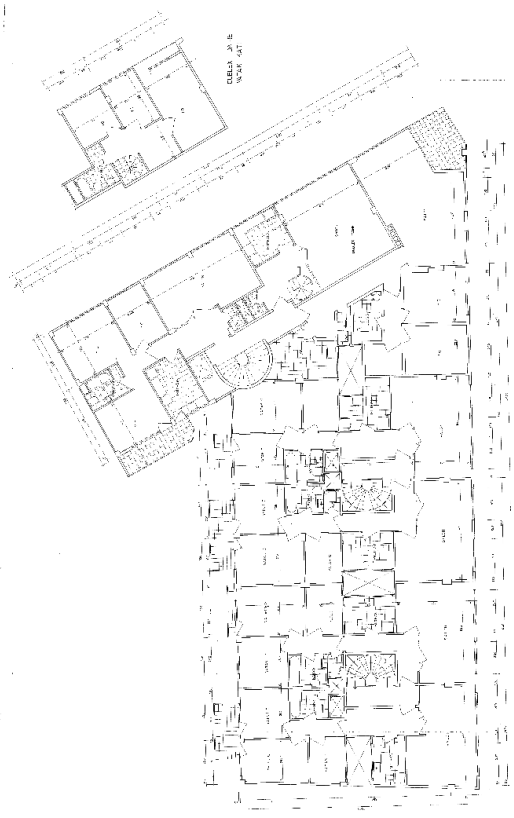

Normal Floor Plan

(f)

Figure 9 Floor Plans (a) 710-31 (b) 757-38 (c) 834-72 (d) 1113-197 (e) 1284-91 (f) 1427-87

3. STRUCTURE MODELING

The first version of the SAP2000 program was introduced to civil engineers in 1996 and provided unlimited use (model creation, development and analysis) with a single Windows compatible interface. It is the most user-friendly version of the SAP series, with interfaces developed since then and new codes added. Since this program has an interface that can solve even the most complex projects, it has been deemed appropriate to be used for static and dynamic analysis. Since the floor plans of the buildings to be modeled have both deficiencies and partial inaccuracies, general or detailed assumptions were made in some cases during modeling; these assumptions, which will not affect the analysis significantly and are very close to reality, are explained in the next section.

3.1 Assumptions for Floor Plans

Since the above-mentioned deficiencies and inaccuracies exist in the floor plans, assumptions have been made on three different issues.

The first of these is the concrete class used. Concrete compressive strength and the flow limit of the reinforcement play an important role in project designing of reinforced concrete structures. If the concrete compressive strength is lower than the concrete compressive strength and yield stress of the reinforcement predicted in practice, it is very important to determine the concrete class used, since there are losses in the bearing capacity of the reinforced concrete elements. Among the selected buildings, there are two buildings with uncertain concrete classes; since the floor plans for the building with the block-parcel number 1427-87 are quite similar and they have the same ground condition, it was decided to use the B225 concrete class used in the other building. In the other building, numbered 757-38, where the concrete class is uncertain, it is assumed that C20 was used, since the C20 concrete class was used at a rate of 49 percent in 2002, according to the Turkish Concrete Association. Table 4 shows the concrete class and construction year of the buildings. As seen in the table, C20 concrete class was used in two of the buildings and B225 concrete class was used in the other four.

Table 4 Concrete classes

	Construction Year	**Concrete Class**
710-31	1976	C20

757-38	2002	C20
834-72	1981	B225(C18)
1113-197	1980	B225(C18)
1284-91	1975	B225(C18)
1427-87	1971	B225(C18)

The second assumption was the dimensions of the columns, although one of the most important things in a plan was the dimensions of the columns, one of the plans (757-38) did not have the dimensions of the columns. Column dimensions, which are the basis of the structural system, were updated by scaling on the column drawings based on the measurements of other data obtained from the physically obtained floor plan, and static analysis was performed after the specified column dimensions were defined; the closeness to reality and accuracy of the static analysis results were tested.

The third assumption is the absence of reinforcement information in buildings numbered 757-38 and 834-72. Since the old earthquake code was used in the years when the buildings were built according to the concrete class and the dimensions of the columns used, by regarding the dimensions of the columns and at the same time the reinforcements used in the other buildings constructed, the missing reinforcement information was obtained as a result of the static calculations made according to the old earthquake code.

3.2. Structural Input Parameters

After the uncertainties in the floor plans were resolved, 3D model drawings were started in the sap2000 program. The floor plans of five of the buildings consist of 3 different plans as basement, floor and normal floor, and one of them consists of 4 different plans as there are 3 different basement plans. Two of the buildings have 6 floors, two have 12 floors, one has 10 floors and the other has 7 floors. These buildings have 12 floors, with one of the two highest buildings being 33400 m and the other 34500 m. The shortest building is 7 floors and 14900 m. Structural input parameters used while making 3D models according to floor plans are shown in Table 5.

Table 5 Floor information

710-31		**757-38**		**834-72**	
Floor	**Level**	**Level**	**Level**	**Floor**	**Level**

Basement	-1700	Basement	-2550	Basement	-12500
Ground	1000	Ground	0	Ground	-8500
1	3700	1	2900	1	-4500
2	6400	2	4900	2	-500
3	9100	3	6900	3	3500
4	11800	4	8900	4	7500
5	14500	5	10900	5	11500
6	17200	6	12900	6	15500
7	19900	7	14900		
8	22600				
9	25300				
10	28000				
11	30700				
12	33400				

(a)

1113-197		**1284-91**		**1427-87**	
Floor	**Level**	**Floor**	**Level**	**Floor**	**Level**
Basement	-1500	Basement	-1900	Basement 3	-10250
1	1500	Ground	1000	Basement 2	-6800
2	4500	1	3900	Basement 1	-3350
3	7500	2	6800	1	100
4	10500	3	9700	2	3550
5	13500	4	12600	3	7000
6	16500	5	15500	4	10450
7	19500	6	18400	5	13900
8	22500	7	21300	6	17350
9	25500	8	24200		
10	28500	9	27100		
11	31500	10	30000		
12	34500				

(b)

3.3. 3D- Model and Modal Analysis

Buildings were modeled in the SAP2000 program according to the building input parameters, floor plans and assumptions. As the floor plans are not similar, the creation of quite different models is important to diversify the results to be obtained in the next stages. Figure 10 shows the building models created in the SAP2000 program.

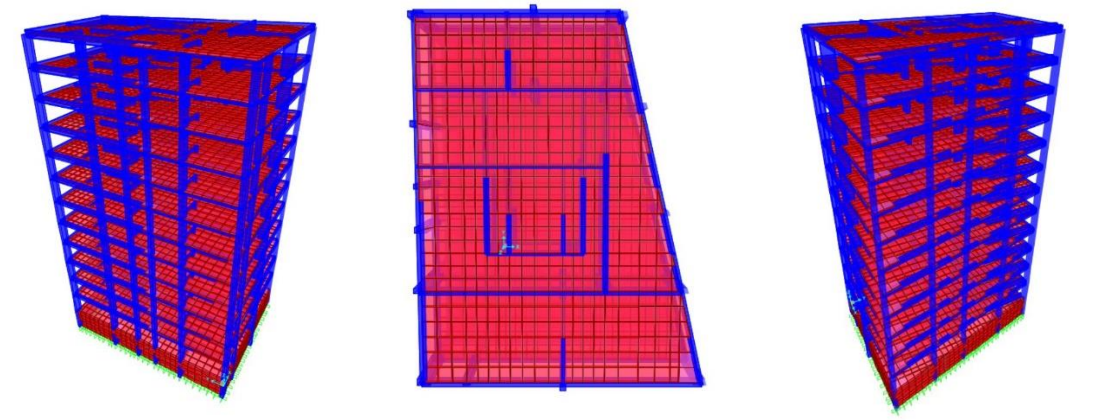

(a)

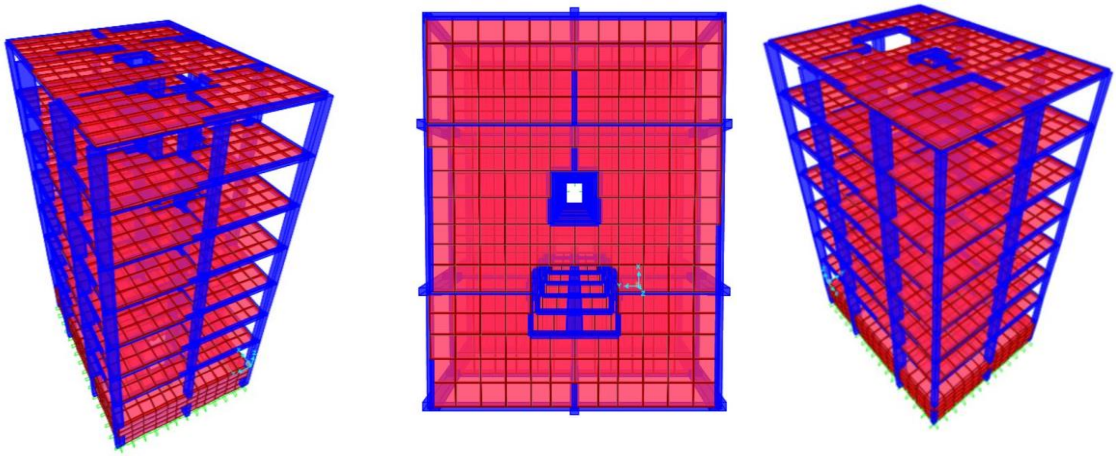

(b)

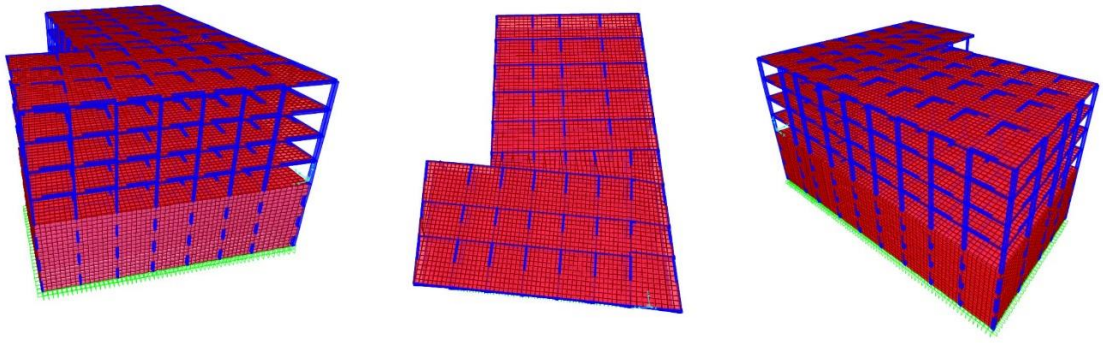

(c)

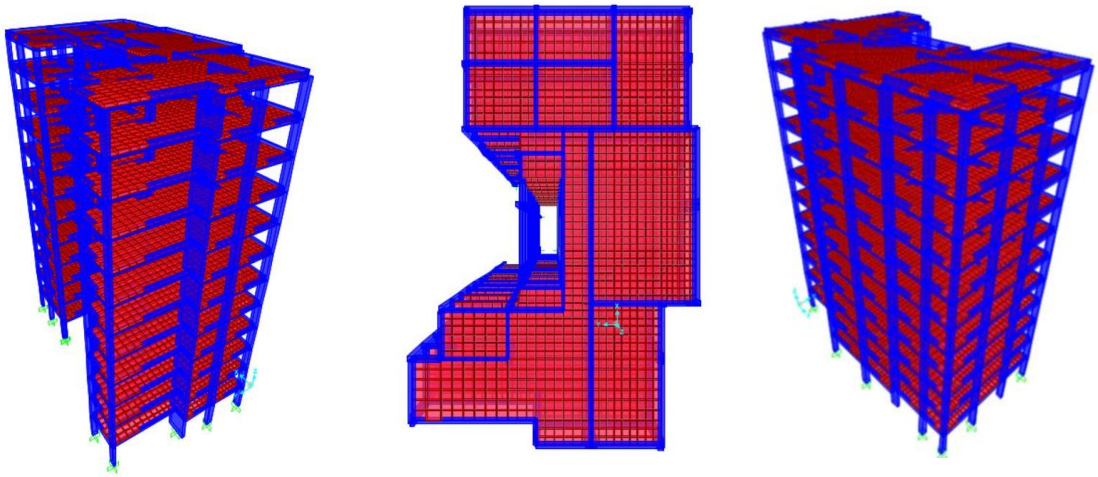

(d)

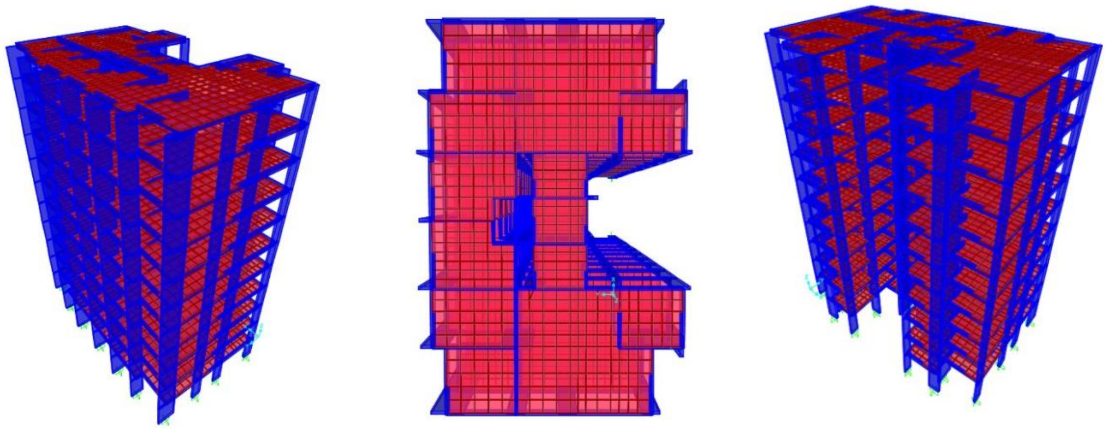

(e)

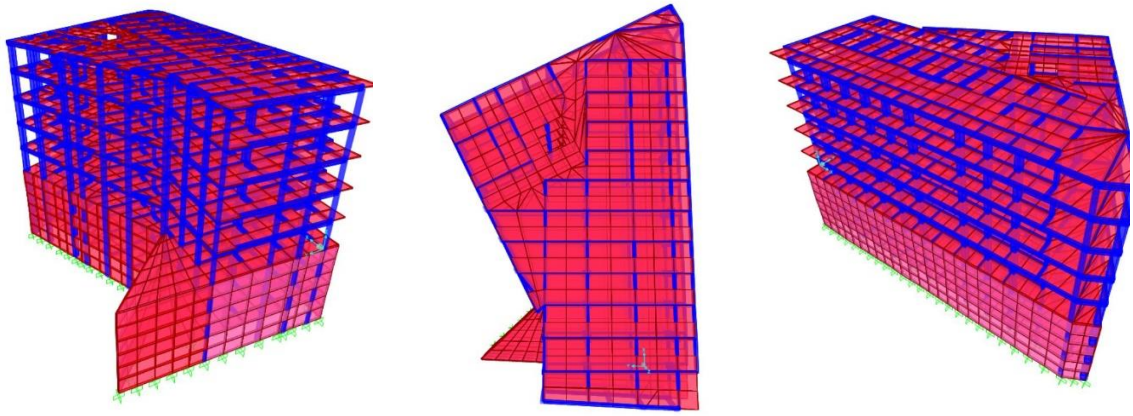

(f)

Figure 10 3D Models (a) 710-31 (b) 757-38 (c) 834-72 (d) 1113-197 (e) 1284-91 (f) 1427-87

In this process, 3D models were created to perform nonlinear time history analyses, but it is very important to select the correct earthquake data in order to bring the analysis results closer to reality; therefore, natural vibration periods of buildings should be determined previously for ground motion selection studies. The most important dynamic feature of the structures is the natural vibration period. The period depends on the weight of the structure and the rigidity of the carrier system against horizontal loads, so the vibration period of multistorey buildings varies according to the number of floors of the structure and the carrier system. The natural vibration periods of the buildings were calculated by conducting modal analysis in the sap2000 program. Figure 11 shows exemplary structure behaviors for a given second from the modal analysis results and table 6 from natural vibration periods.

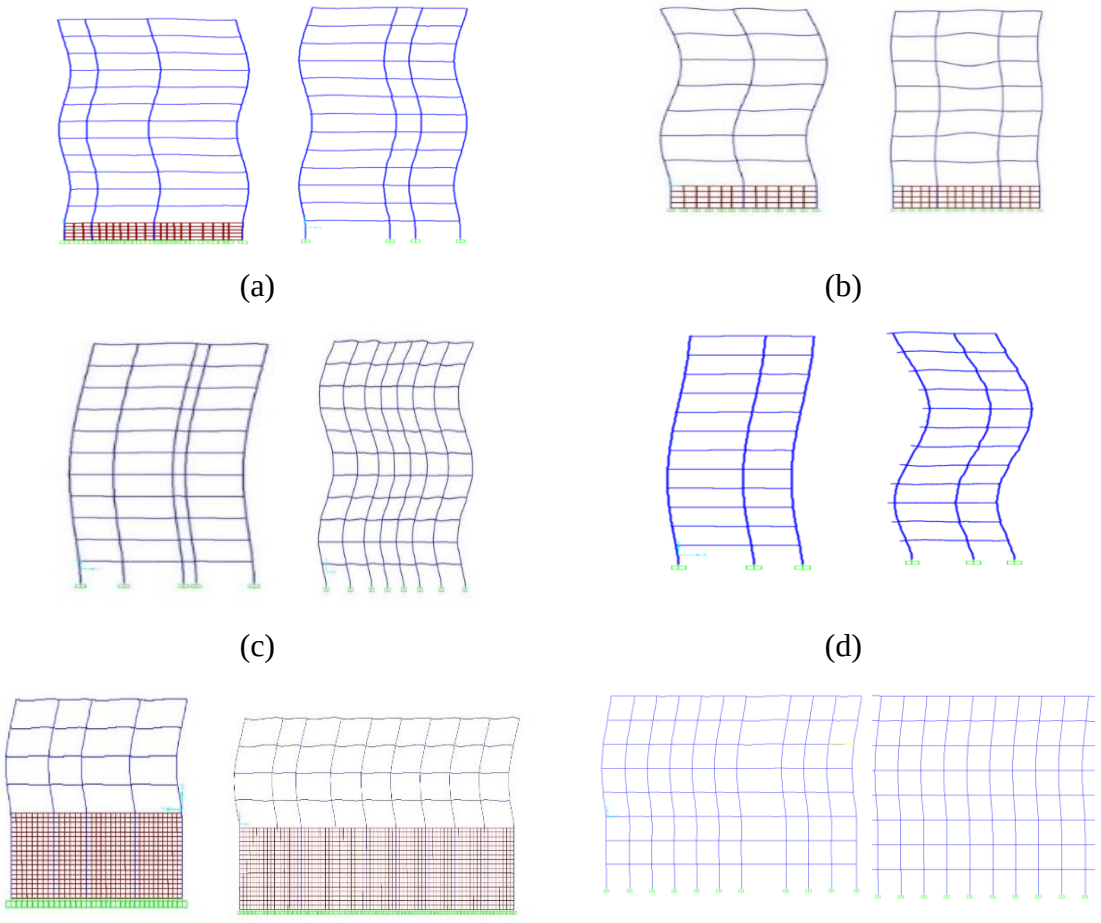

(a) (b)

(c) (d)

(e) (f)

Figure 11 Modal Analysis (a) 710-31 (b) 757-38 (c) 834-72 (d) 1113-197 (e) 1284-91 (f) 1427-87

Table 6 Natural vibration periods of buildings.

	Natural Vibration Periods (s)
710-31	1.05
757-38	0.91
834-72	1.029
1113-197	1.24
1284-91	1.098
1427-87	0.62

4. GROUND MOTION

In order to perform nonlinear time history analysis of the buildings modeled in the SAP2000 program, the ground motions to be analyzed should be selected and scaled according to the behavior of the building.

4.1. Parcel Information for Structures

In the selections of earthquake records, first of all, the design spectra of the buildings should be drawn, and in order to select the real ground motions, the design spectra of the buildings should be created first. Before the selection and scaling processes, the design spectra for the 2475-year return period were created by taking the Turkish Earthquake Code as a reference according to the latitude and longitude of the buildings.

Once the design spectrum has been determined, the hazard spectrum must be generated and compared with the design spectrum to determine the target spectrum. Hazard spectra were plotted using the OpenQuake computer program, assuming Vs30 (Average shear wave velocity) and Z1.0 (1.0 km⁄s shear wave velocity) [29] values as the basic parameter. The Z1.0 values of the buildings were determined according to equation (1), and the Vs30 values were determined according to the map shown in Figure 12 prepared by the Istanbul Municipality [24]. Table 7 shows the average shear wave velocity value ranges according to the colors of the map in figure 7. Table 8 shows the Vs30 and Z1.0 values of the buildings.

$$ln(Z_{1.0}) = \frac{-7.15}{4} l\,n\left(\frac{V_{S30}^4 + 571^4}{1336^4 + 571^4}\right) \quad (1)$$

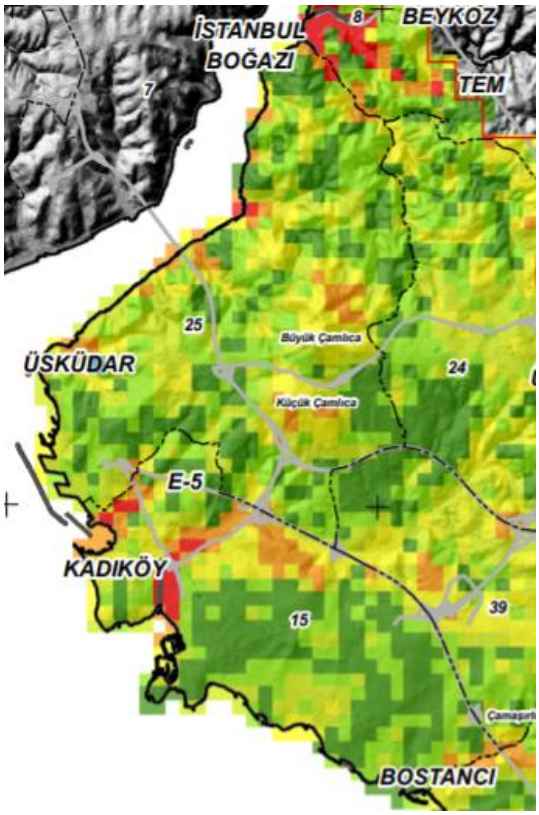

Figure 12 Map of V_{s30} (Average shear wave velocity), revisited from Istanbul Municipality [25]

Table 7 Legend for figure 7

	Vs Average Shear Wave Velocity (m/s)
	0 m/s < Vs_{30} <= 300 m/s
	300 m/s < Vs_{30} <=450 m/s
	450 m/s < Vs_{30} <= 600 m/s
	600 m/s < Vs_{30} <= 700 m/s
	700 m/s < Vs_{30} <= 800 m/s
	800 m/s < Vs_{30} <= 1500 m/s

Table 8 Vs_{30} and $Z_{1.0}$ values of the buildings

		Latitude	**Longitude**	**Vs_{30}(m/s)**	**ln$Z_{1.0}$**	**$Z_{1.0}$**
PA	**710-31**	40.97389	29.04528	700	4.148238	63.32231

	757-38	40.97194	29.04694	800	3.436248	31.07015
	834-72	40.98944	29.02278	700	4.148238	63.32231
	1113-197	40.97389	29.0425	700	4.148238	63.32231
	1284-91	40.97417	29.05944	700	4.148238	63.32231
	1427-87	40.99194	29.02944	450	5.676675	291.977

4.2. Construction of Design Spectrum and Hazard Spectrum

In order for the natural vibration periods of the buildings to affect the selection of the real earthquake record, the determination of the target spectrum was continued with the calculations of the hazard spectrum. The hazard spectra of the buildings were obtained using the OpenQuake open-source program; design spectra were calculated according to the Turkish Building Earthquake Code. Table 9 shows the ground class of the buildings according to the Turkish Building Earthquake Code. In order to show the suitability of the use of the hazard spectrum, the design spectra and the hazard spectra were compared and according to the comparison result, it was shown that the hazard spectra could be used instead of the design spectra. Figure 13 shows the comparison between the design spectra and the hazard spectra.

Table 9 Soil Class for Building

	710-31	**757-38**	**834-72**	**1113-197**	**1284-91**	**1427-87**
Latitude	40.9739	40.9719	40.9894	40.9739	40.9742	40.9919
Longitude	29.0453	29.0469	29.0228	29.0425	29.0594	29.0294
S_S(g) 475 Return period	1.01	1.015	0.984	1.013	0.995	0.97
S_S(g) 2475 Return period	1.754	1.762	1.71	1.759	1.729	1.685
S_1(g) 475 Return period	0.275	0.276	0.27	0.276	0.271	0.266
S_1(g) 2475 Return period	0.487	0.489	0.476	0.488	0.479	0.469
Local Soil Class	ZB	ZC	ZD	ZB	ZB	ZC

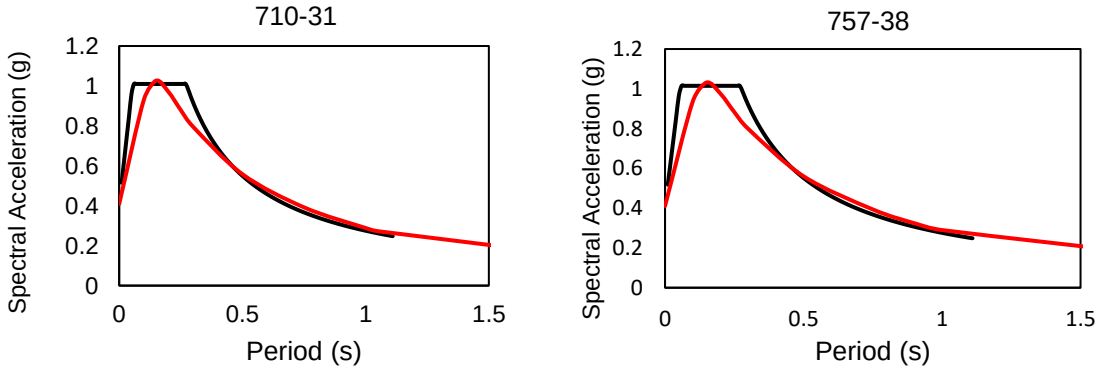

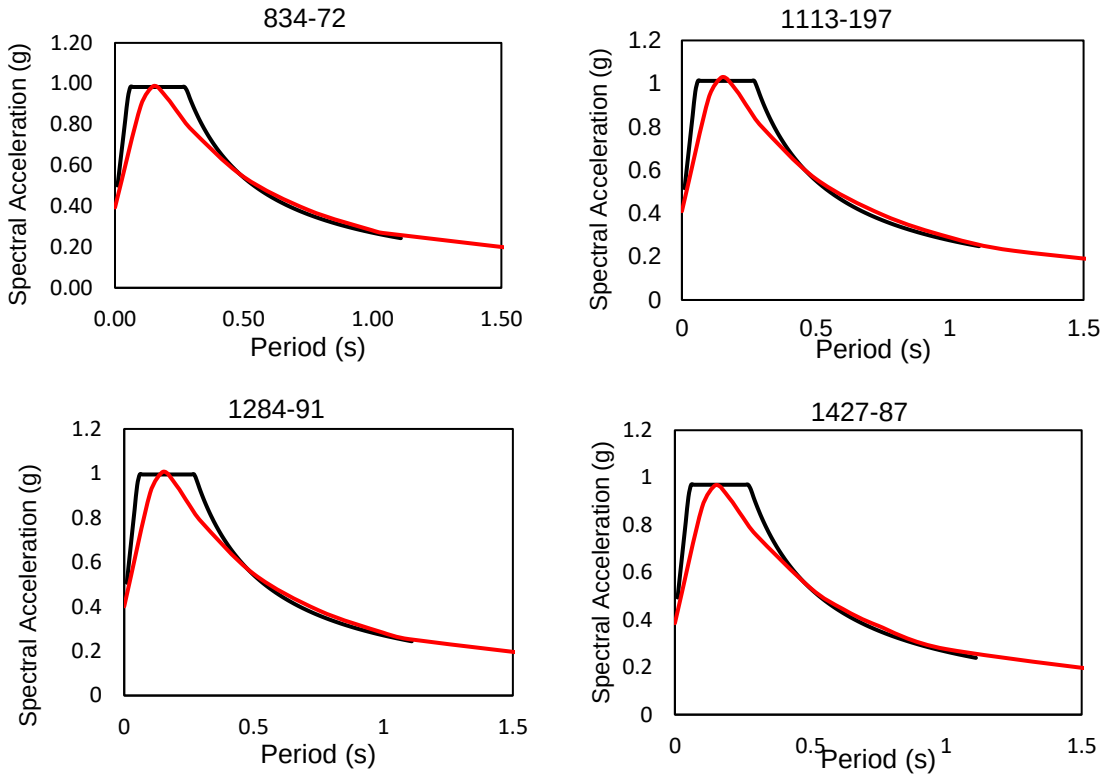

Figure 13 Design Spectra and Hazard Spectra Curves (Black lines: Desing spectra, Red lines: Hazard spectra)

4.3. Deaggregation Process

Probabilistic seismic hazard analysis (PSHA) combines the probabilities of all earthquake scenarios of different magnitudes and distances with the resulting ground motion intensity estimates to calculate the seismic hazard at a site. PSHA also combines uncertainties in ground motion predictions by considering multiple Ground Motion Prediction Models (GMPMs). The current ground motion selection uses probabilistic seismic hazard deaggregation to determine the distribution of earthquake scenarios that contribute to exceeding a given spectral acceleration (Sa). The most effective earthquake scenario for the investigated structures can only be defined by deaggregation. For the ground motion selection process, the reference ranges in which the earthquake parameters (Magnitude, Mw, Joyner-Boore Distance, RJB) are most effective should be determined; in this study, reference ranges of earthquake parameters that affect the structures the most were obtained by deaggregation process by means of OpenQuake computer program. The most effective earthquake scenario was determined by regarding the maximum exceedance probability values for each building. According to the results of the deaggregation process, 6.5M

magnitude and 15 kilometers Joyner-Boore distances were determined as the scenario causing the most effect for the 6 buildings selected. Figure 14 shows the results of the deaggregation process.

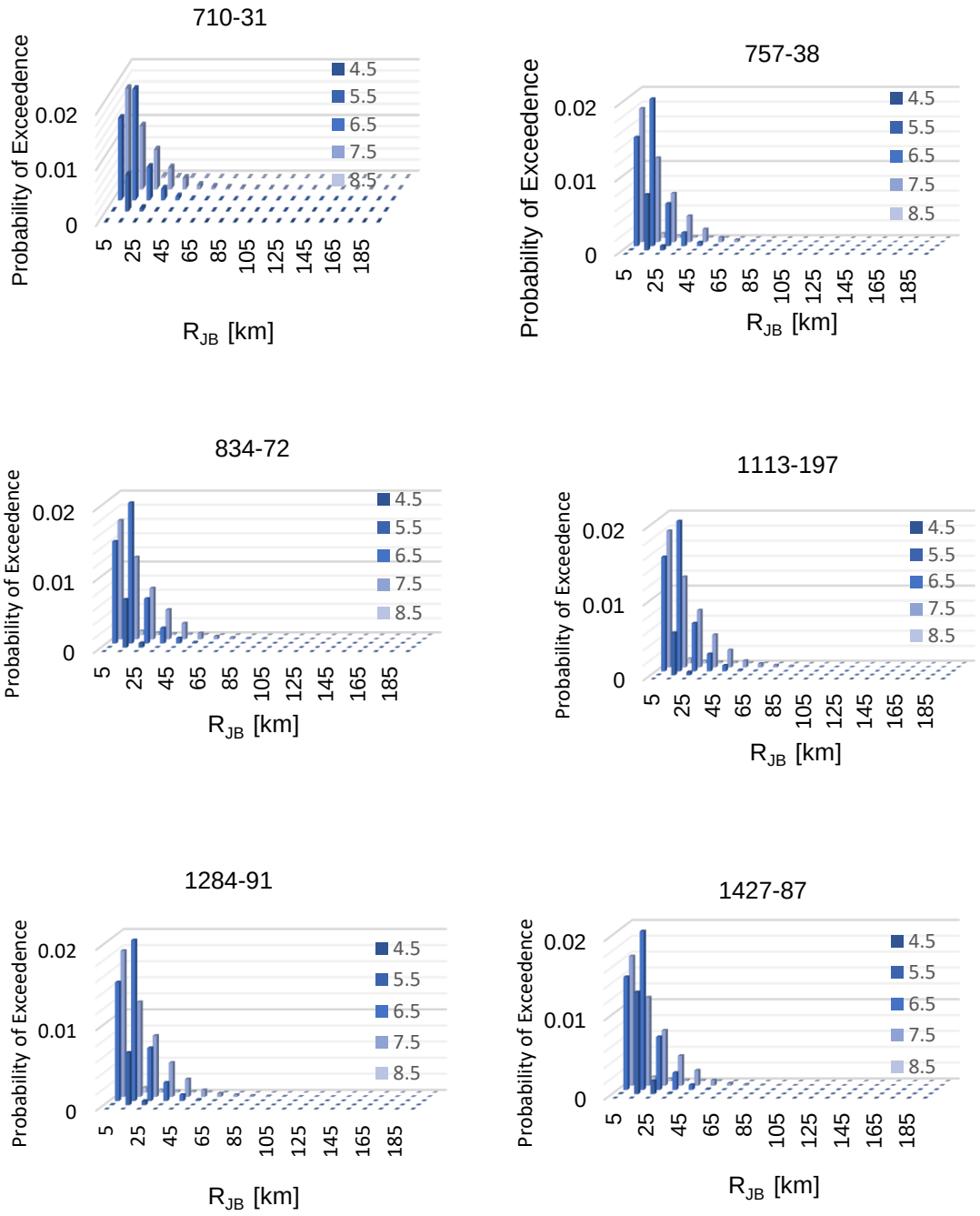

Figure 14 Deaggregation process

4.4. Obtaining Ground Motion Records

According to the deaggregation results, the first 3 earthquake scenarios with the highest exceedance probability were determined for each building and 4 different groups were determined, a total of 18 earthquake scenarios for 6 buildings. Ground motion records as 4 different earthquake parameter sets were downloaded from the PEER (Pacific Earthquake Engineering Research Center) website. First set was determined as 6-7M for Mw, 0-20 kilometers for RJB and 600-900m/s for VS30, second set as 7-8M for Mw, 0-30 kilometers for RJB and 600-900m/s for VS30, third set as 6-7M for Mw, 0-20 kilometers for RJB and 400-500 m/s for VS30 and fourth set as 7-8M for Mw, 0-30 kilometers for RJB and 400-500 m/s for VS30. Table 10 shows the earthquake parameter ranges of the sets created for the records downloaded from the PEER website.

Table 10 Record Sequence Numbers of Downloaded Records

	M_w(M)	R_{JB}(m)	V_{S30}(m/s)
Set I	6,7	0,20	600,900
Set II	7,8	0,30	600,900
Set III	6,7	0,20	400,500
Set IV	7,8	0,30	400,500

4.5. Construction of Conditional Spectrum and Target Spectrum

It is very important to determine the target spectrum for the correct selection of ground movements. The target spectrum was estimated using 4 different methods in the study of Lin et al. [26]. In this study, method 2 (Approximate CS Using Mean M/R) and method 4 (Logic Tree Weighted GMPMs) were compared. As a result of the comparison, when the curves obtained using both method 2 and method 4 are examined, it is seen that there is no effect that will make a difference on the selection of ground motion, and since the 4 different most effective earthquake scenarios are used in method 4, this method has been preferred to be used. Figure 15 shows the target spectrum curves generated using method 2 and method 4. The conditional spectrum in Method 4 was calculated according to the studies of Akkar et

al. (2014) [27], Kale et al. (2015) [28], Boore et al. (2014) [29] and Chiou and Youngs et al. (2014) [30] using four different 0.25-weighted mean and standard deviation values.

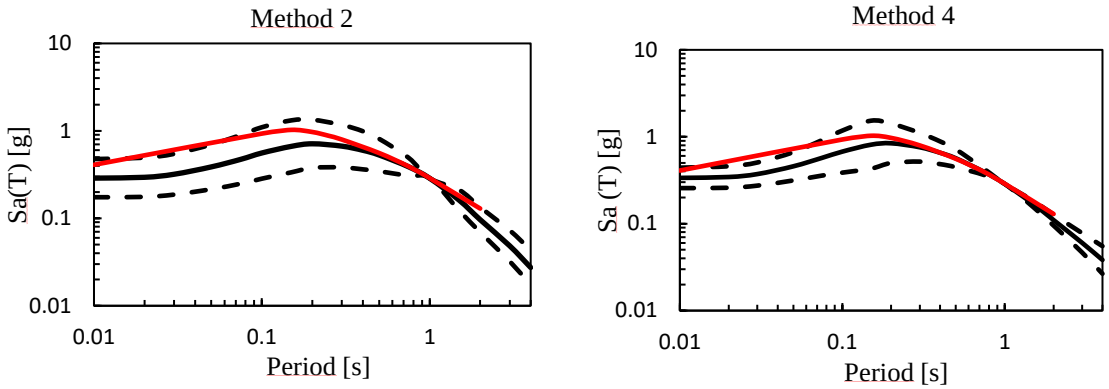

Figure 15 Comparison of Method 2 and Method 4 (Black dashed lines are μ – σ and μ + σ curves, black line is conditional mean curve, orange lines are target spectra)

4.6. Ground Motion Selection and Scaling

The selected real earthquake records are scaled according to the Sae value in the natural vibration periods of the buildings. In order to select the correct records, the x-axis in the period vs. Sae graph has been updated to be in the range of 02T-1.5T. T denotes the natural vibration period of each building and thirty different records were selected that fall between the μ - σ and μ + σ curves, Figure 16 shows the μ - σ and μ + σ curves. (Black dashed lines are μ – σ and μ + σ curves, black lines are conditional mean curves, gray lines are downloaded records). Table 11 shows the recording sequence numbers of the selected recordings in PEER, Table 12 shows the characteristic features of the selected ground motion.

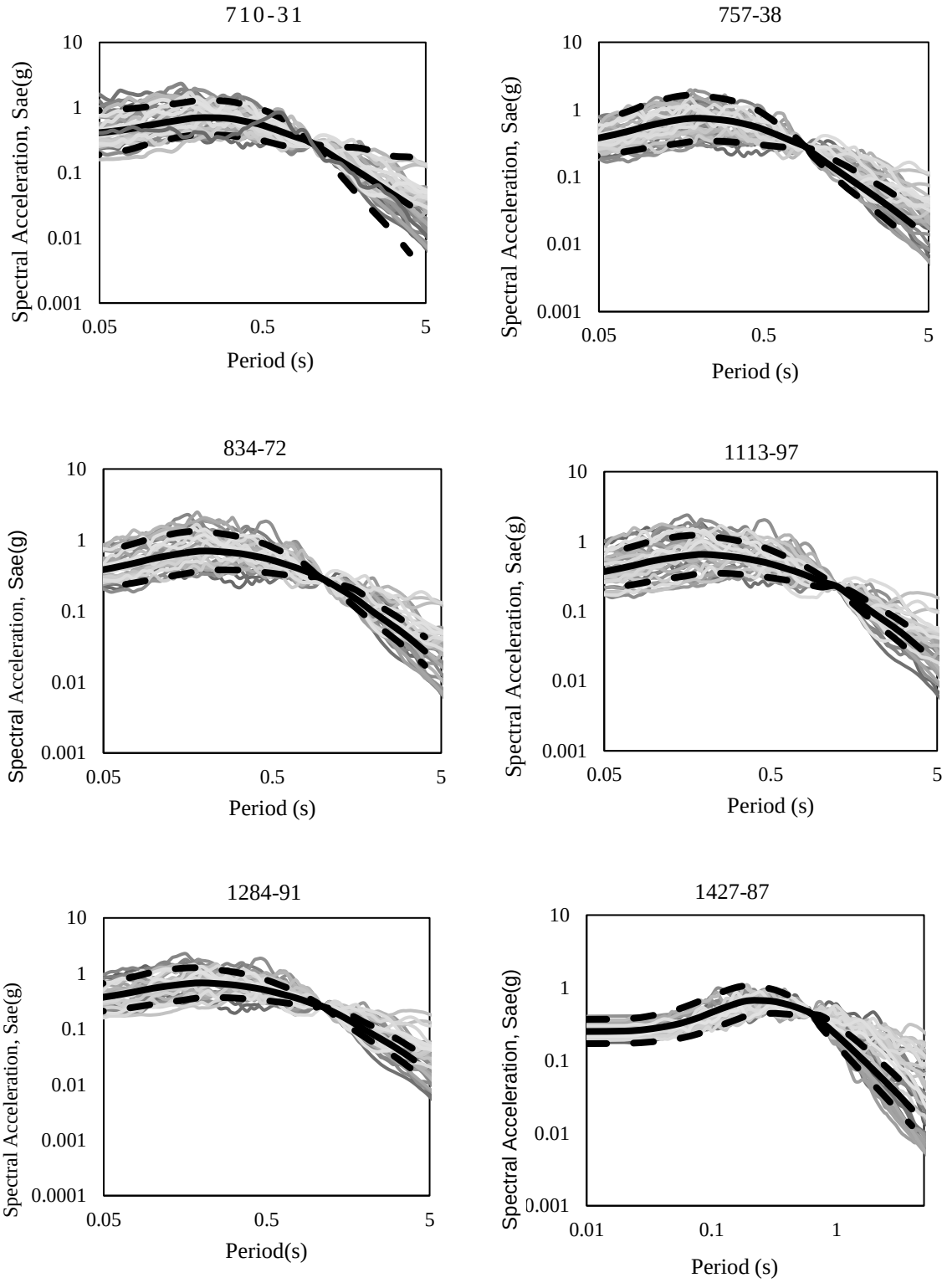

Figure 16 Selected Earthquake Records

Table 11 Record Sequence Number of Selected Earthquake Records

	Selected Records (RSN)
710-31	72, 143, 296, 769, 801, 989, 1012, 1013, 1078, 1161, 1485, 1507, 1511, 1521, 1613, 1618, 1633, 1787, 2627, 2635, 3943, 4472, 4475, 4481, 4483, 4843, 4864, 4876, 6928, 8164
757-38	72, 143, 296, 763, 769, 801, 1012, 1078, 1111, 1126, 1485, 1507, 1521, 1618, 1633, 1787, 2635, 3943, 4284, 4472, 4475, 4481, 4483, 4842, 4843, 4864, 5618, 6928, 8110, 8164
834-72	72, 143, 296, 801, 989, 1012, 1078, 1126, 1161, 1485, 1507, 1511, 1521, 1613, 1618, 1633, 1787, 2627, 3943, 4472, 4475, 4481, 4483, 4843, 4864, 4876, 5809, 6928, 8110, 8164
1113-197	143, 296, 459, 763, 769, 801, 989, 1012, 1078, 1161, 1234, 1485, 1507, 1511, 1521, 1613, 1618, 1633, 1787, 2627, 2635, 3943, 4472, 4475, 4481, 4483, 4843, 4864, 6928, 8164
1284-91	72, 285, 296, 763, 769, 801, 809, 989, 1012, 1013, 1078, 1161, 1485, 1507, 1511, 1521, 1551, 1613, 1618, 2627, 2635, 3943, 4472, 4475, 4481, 4483, 4843, 4864, 4876, 5809
1427-87	57, 139, 164, 284, 289, 741, 753, 1086, 1208, 1476, 1486, 1493, 1512, 1546, 2628, 2655, 2699, 3473, 3746, 4031, 4103, 4139, 4144, 4147, 4148, 4149, 4219, 4285, 4457, 4480

Table 12 Characteristic features of selected ground motion.

Earthquake Name	Year	Station Name	Magnitude	Mechanism	R_{JB} (km)	V_{s30} (m/sec)	Record RSN Number
"San Fernando"	1971	"Castaic - Old Ridge Route"	6.61	Reverse	19.33	450.28	RSN57
"San Fernando"	1971	"Lake Hughes #4"	6.61	Reverse	19.45	600.06	RSN72
"Tabas_ Iran"	1978	"Dayhook"	7.35	Reverse	0	471.53	RSN139
"Tabas_ Iran"	1978	"Tabas"	7.35	Reverse	1.79	766.77	RSN143
"Imperial Valley-06"	1979	"Cerro Prieto"	6.53	strike slip	15.19	471.53	RSN164
"Irpinia_ Italy-01"	1980	"Auletta"	6.9	Normal	9.52	476.62	RSN284
"Irpinia_ Italy-01"	1980	"Bagnoli Irpinio"	6.9	Normal	8.14	649.67	RSN285
"Irpinia_ Italy-01"	1980	"Calitri"	6.9	Normal	13.34	455.93	RSN289
"Irpinia_ Italy-02"	1980	"Bagnoli Irpinio"	6.2	Normal	17.79	649.67	RSN296
"Morgan Hill"	1984	"Gilroy Array #6"	6.19	strike slip	9.85	663.31	RSN459
"Nahanni_ Canada"	1985	"Site 1"	6.76	Reverse	2.48	605.04	RSN495
"Nahanni_ Canada"	1985	"Site 2"	6.76	Reverse	0	605.04	RSN496
"Loma Prieta"	1989	"BRAN"	6.93	Reverse Oblique	3.85	476.54	RSN741
"Loma Prieta"	1989	"Corralitos"	6.93	Reverse Oblique	0.16	462.24	RSN753

"Loma Prieta"	1989	"Gilroy - Gavilan Coll."	6.93	Reverse Oblique	9.19	729.65	RSN763
"Loma Prieta"	1989	"Gilroy Array #6"	6.93	Reverse Oblique	17.92	663.31	RSN769
"Loma Prieta"	1989	"San Jose - Santa Teresa Hills"	6.93	Reverse Oblique	14.18	671.77	RSN801
"Loma Prieta"	1989	"UCSC"	6.93	Reverse Oblique	12.15	713.59	RSN809
"Northridge-01"	1994	"LA - Chalon Rd"	6.69	Reverse	9.87	740.05	RSN989
"Northridge-01"	1994	"LA 00"	6.69	Reverse	9.87	706.22	RSN1012
"Northridge-01"	1994	"LA Dam"	6.69	Reverse	0	628.99	RSN1013
"Northridge-01"	1994	"Santa Susana Ground"	6.69	Reverse	1.69	715.12	RSN1078
"Kobe_ Japan"	1995	"Nishi-Akashi"	6.9	strike slip	7.08	609	RSN1111
"Kozani_ Greece-01"	1995	"Kozani"	6.4	Normal	14.13	649.67	RSN1126
"Kocaeli_ Turkey"	1999	"Gebze"	7.51	strike slip	7.57	792	RSN1161
"Chi-Chi_ Taiwan"	1999	"TCU089"	7.62	Reverse Oblique	0	671.52	RSN1521
"Chi-Chi_ Taiwan"	1999	"TCU138"	7.62	Reverse Oblique	9.78	652.85	RSN1551
"Duzce_ Turkey"	1999	"Lamont 531"	7.14	strike slip	8.03	638.39	RSN1618
"Manjil_ Iran"	1990	"Abbar"	7.37	strike slip	12.55	723.95	RSN1633
"Hector Mine"	1999	"Hector"	7.13	strike slip	10.35	726	RSN1787

"Chi-Chi_ Taiwan-03"	1999	"TCU076"	6.2	Reverse	13.04	614.98	RSN2627
"Chi-Chi_ Taiwan-03"	1999	"TCU089"	6.2	Reverse	5.93	671.52	RSN2635
"Tottori_ Japan"	2000	"SMN015"	6.61	strike slip	9.1	616.55	RSN3943
"Parkfield-02_ CA"	2004	"Slack Canyon"	6	strike slip	1.6	648.09	RSN4097
"Basso Tirreno_ Italy"	1978	"Naso"	6	strike slip	17.15	620.56	RSN4284
"L'Aquila_ Italy"	2009	"Celano"	6.3	Normal	17.82	612.78	RSN4472
"L'Aquila_ Italy"	2009	"Fiamignano"	6.3	Normal	19.08	638.39	RSN4475
"L'Aquila_ Italy"	2009	"L'Aquila - V. Aterno -Colle Grilli"	6.3	Normal	0	685	RSN4481
"L'Aquila_ Italy"	2009	"L'Aquila - Parking"	6.3	Normal	0	717	RSN4483
"Chuetsu-oki_ Japan"	2007	"Joetsu Uragawaraku Kamabucchi"	6.8	Reverse	18.6	655.45	RSN4842
"Chuetsu-oki_ Japan"	2007	"Matsushiro Tokamachi"	6.8	Reverse	18.16	640.14	RSN4843
"Chuetsu-oki_ Japan"	2007	"Yoitamachi Yoita Nagaoka"	6.8	Reverse	4.69	655.45	RSN4864
"Chuetsu-oki_ Japan"	2007	"Kashiwazaki Nishiyamacho Ikeura"	6.8	Reverse	0	655.45	RSN4876
"Iwate_ Japan"	2008	"Minase Yuzawa"	6.9	Reverse	17.34	655.45	RSN5809
"Christchurch_ New Zealand"	2011	"MQZ"	6.2	Reverse Oblique	13.91	649.67	RSN8110
"Duzce_ Turkey"	1999	"IRIGM 487"	7.14	strike slip	2.65	690	RSN8164

5. ANALYSIS CONSIDERATIONs

After selecting the ground motion records, the uniform hazard spectrum was determined as the target spectrum in the SeismoMatch program according to the exceedance probability values corresponding to 5 different return periods, and the real earthquake data of each ground motion record was matched. In the matches, the target spectrum and the ground motion recording matched 90 percent and more. Table 13 shows the exceedance probability values corresponding to the selected return periods.

Table 13 Probability of exceedance values corresponding to the selected return periods.

Return Period	Probability of Exceedance
72	0.5
475	0.1
975	0.05
2475	0.02
4975	0.01

5.1. Nonlinear Time History Analysis

After the matching was completed, nonlinear time history analyses were started on the models prepared in the sap2000 program to obtain the fragility curves. Since there are 60 different records with 5 different exceedance probability values for each building, nonlinear time history analysis was performed for 300 records in each building. In other words, a total of 1800 nonlinear time history analyses were performed. The ground motion records selected in the Sap2000 program were defined as functions and the analyses were completed successfully. Figure 17 shows six of the 1800 results obtained for different exceedance probability values for each building.

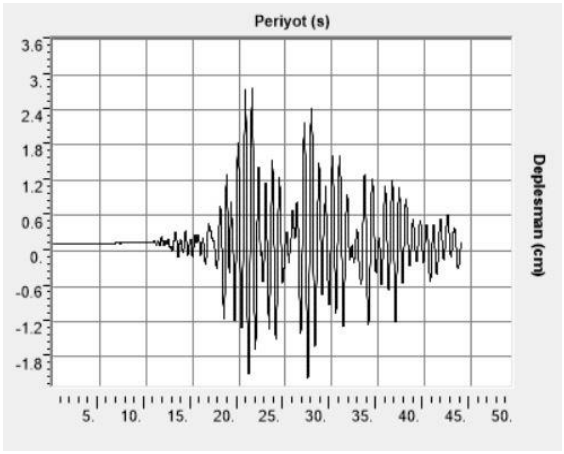

(a)

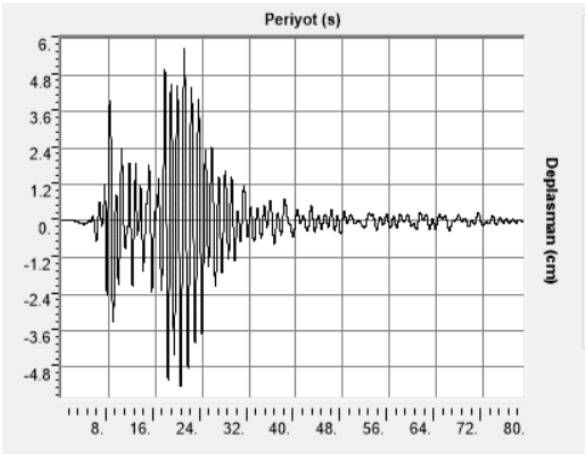

(b)

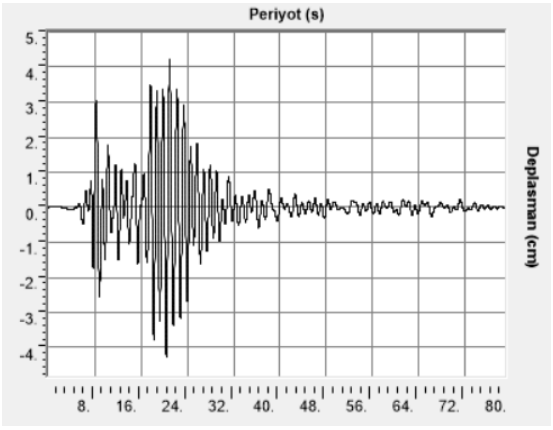

(c)

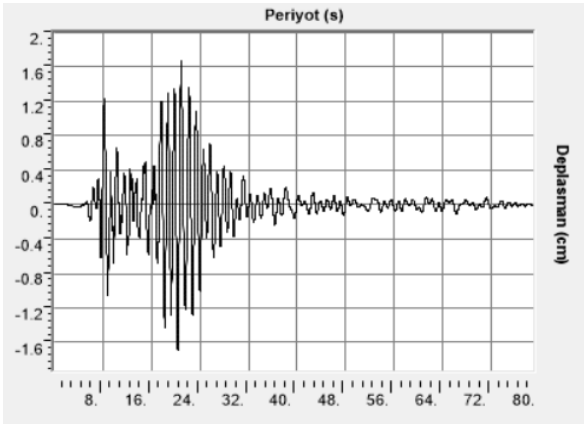

(d)

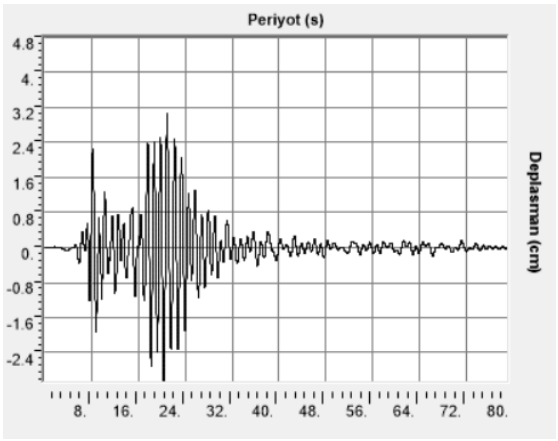

(e)

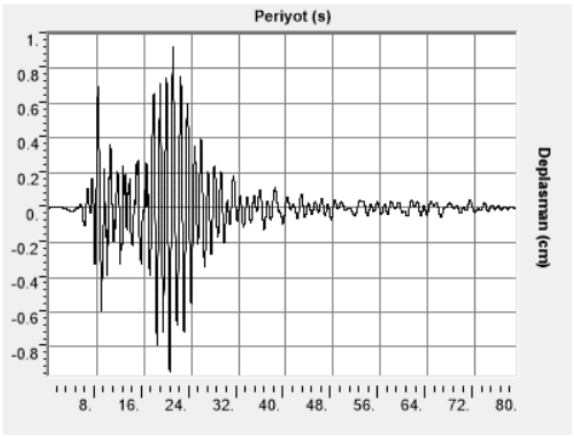

(f)

Figure 17 Time History Analysis Results (a)710-31 (b) 757-38 (c) 834-72 (d) 1113-197 (e) 1284-91 (f) 1427-87

5.2. Story Displacement

The definition of collapse for buildings is not unique since different codes and authors define it according to different engineering failure parameters. Since collapse is associated with large plastic deformations, collapse is typically defined by the parameters of deformation, displacement, and ultimately energy engineering failure. In this study, it was determined whether the buildings collapsed by using the roof displacements as the failure parameter.

Roof displacement values obtained by nonlinear time history analysis with 300 different ground motion records for each building are listed according to the maximum displacement value. Analysis of the smallest exceedance probability (0.001) resulted in the highest displacement values. Whether the buildings collapsed or not was determined by the roof displacement values greater than 0.1 times the total height of the building.

The normal distribution curves of the roof displacement values obtained for 5 different exceedance probability values selected according to the results of 300 nonlinear time history analyses of the buildings are shown in Figure 18.

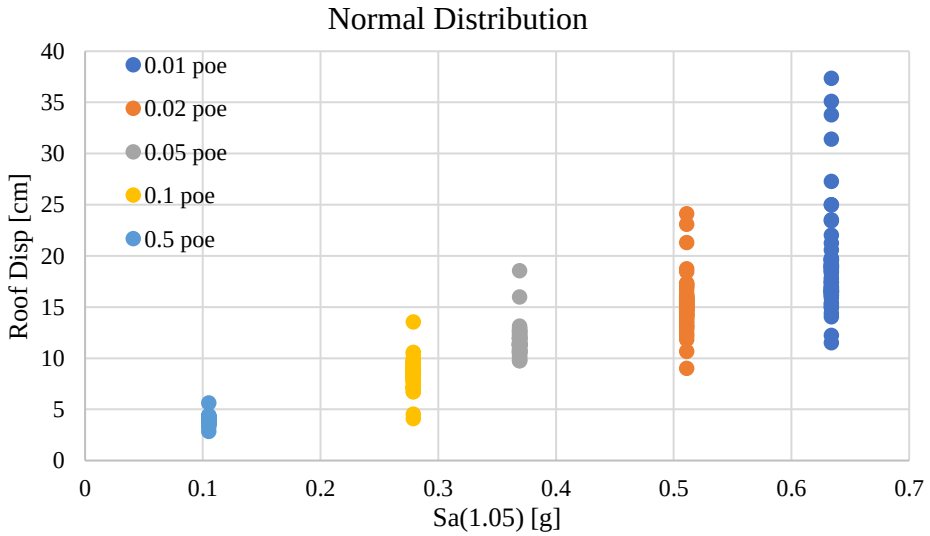

(a)

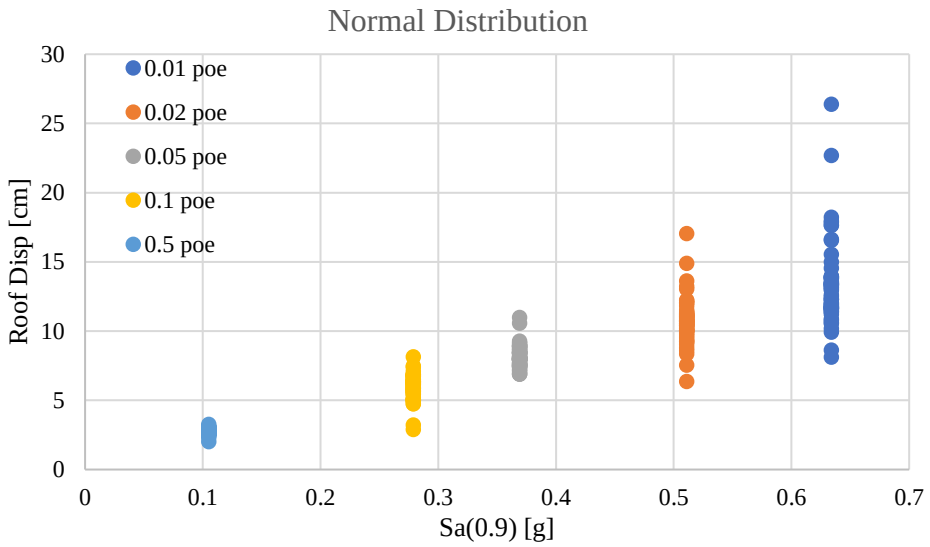
Normal Distribution
0.01 poe
0.02 poe
0.05 poe
0.1 poe
0.5 poe
Roof Disp [cm]
Sa(0.9) [g]
0
5
10
15
20
25
30
0
0.1
0.2
0.3
0.4
0.5
0.6
0.7

(b)

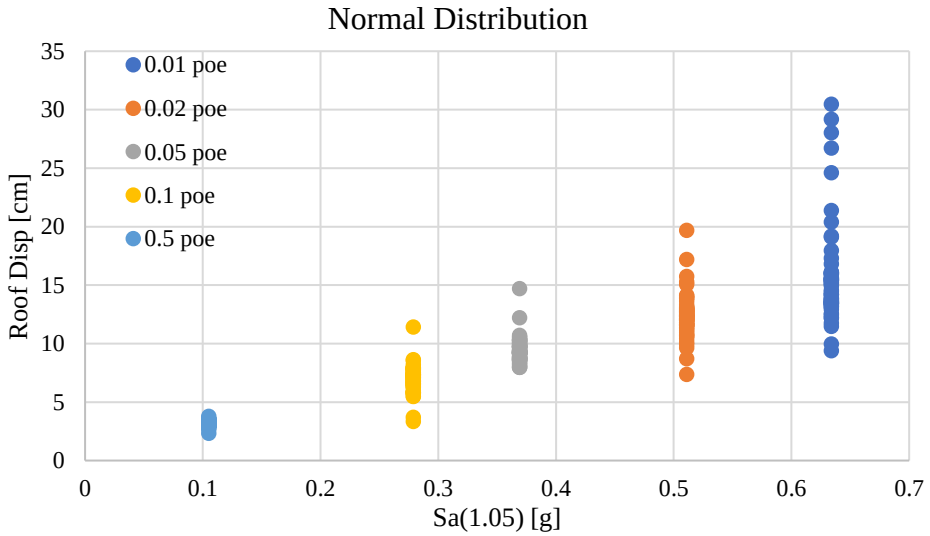
Normal Distribution
0.01 poe
0.02 poe
0.05 poe
0.1 poe
0.5 poe
Roof Disp [cm]
Sa(1.05) [g]
0
5
10
15
20
25
30
35
0
0.1
0.2
0.3
0.4
0.5
0.6
0.7

(c)

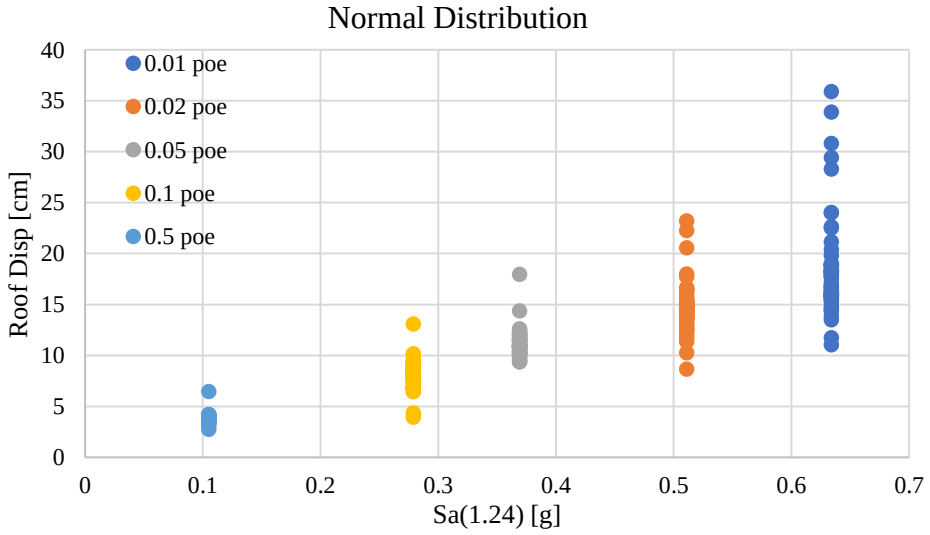
Normal Distribution
0.01 poe
0.02 poe
0.05 poe
0.1 poe
0.5 poe
Roof Disp [cm]
Sa(1.24) [g]
0
5
10
15
20
25
30
35
40
0
0.1
0.2
0.3
0.4
0.5
0.6
0.7

(d)

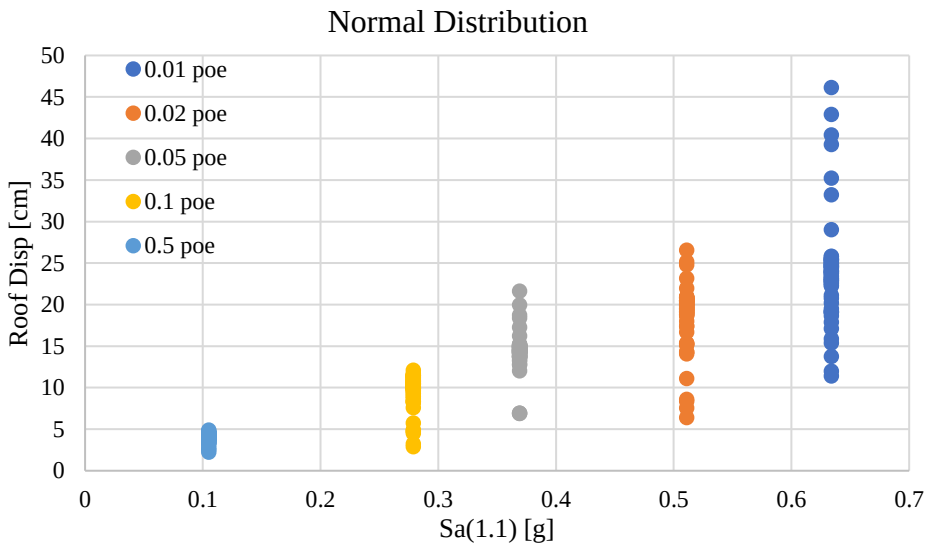

(e)

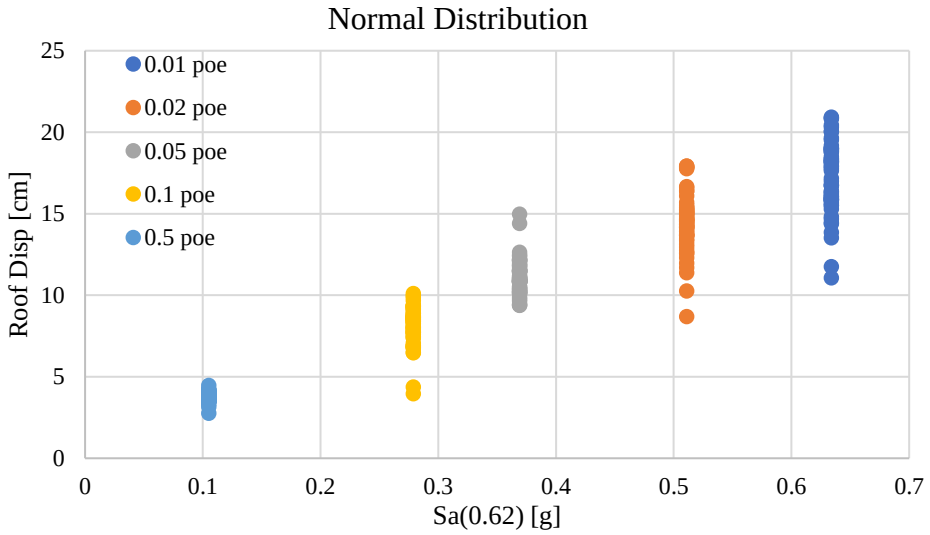

(f)

Figure 18 Normal distribution graphs (a) 710-31 (b) 757-38 (c) 834-72 (d) 1113-197 (e) 1284-91 (f) 1427-87

6. FRAGILITY CURVE

A fragility curve represents the probability that the response of a given structure to various loading conditions will exceed a certain performance limit state, so a fragility curve can be a conditional probability or specific damage corresponding to a structure for a given hazard level exceeding the level. Therefore, fragility curves are a measure of performance with probability terms. Fragility curves are emerging as a useful engineering tool in risk assessment, and also fragility curves are important for estimating the risk caused by possible earthquakes and predicting the economic effects for future earthquakes. They can be used by national institutions for emergency response and disaster planning, and by insurance companies to estimate overall loss after an earthquake. In addition, still fragility curves can be used to reduce risk by improving seismic codes. In this study, fragility curves were obtained to be used as input to the created Markov decision process application. In other words, the obtained curves will be used as inputs for re-electrification in both an economic and a vital system.

6.1. Analytical Steps of Fragility Analysis

Fragility curves can be derived using analytical methods or from empirical data obtained from real events. In this study, fragility curves were obtained by following analytical steps. Figure 19 shows the analytical steps of the fragility analysis used in this study.

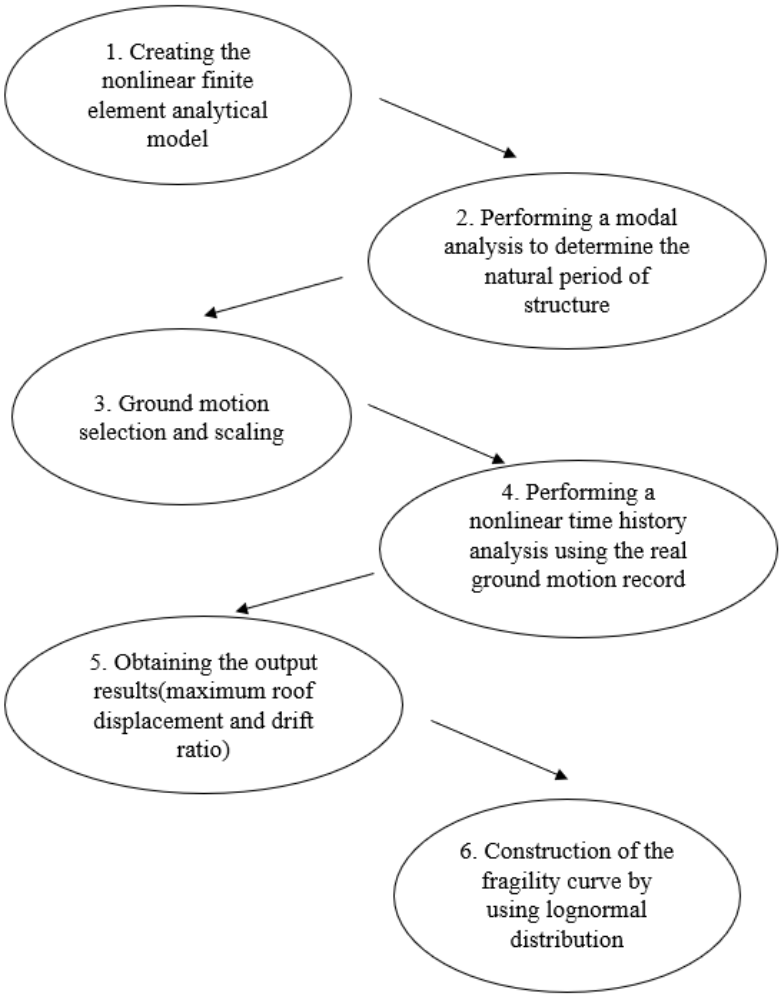

Figure 19 Analytical steps of fragility analysis

6.2. Parameters Effect on Fragility

In this study, every step described up to this point has been done in order to obtain fragility curves. In other words, every parameter used and every calculated value affects the exceedance probability that these curves indicate; but the effect rates are different. The number of floors, floor plan, location and used ground parameters of the building are the factors that affect the result the most. These are described in detail in sections 2 and 3. Considering the 6 different curves that will emerge and the buildings they represent, it is clearly seen which parameter is more effective.

6.3. Construction of Fragility Curve

The most common form (but not universal, best, always appropriate, etc.) of the seismic fragility function is the lognormal cumulative distribution function (CDF). This form is shown in equation 2. The roof displacement data obtained as a result of 1800 nonlinear time history analysis were used as input to the lognormal cumulative distribution function,

$$F(x) = \Phi\left(\frac{ln(x-\mu)}{\sigma}\right) \quad (2)$$

Where;

x: a particular value for roof displacement

F_ (x): a fragility function

Φ(s): standard normal cumulative distribution function (often called the Gaussian)

μ: mean value of max roof displacement for building.

σ: the standard deviation of max roof displacement for building.

The roof displacement values obtained from the nonlinear time history analysis results of the building numbered 1284 were used as input in the Lognormal distribution function, and a point representation fragility curve was obtained. Figure 20 shows the dotted representation fragility curve of 1284 obtained using the lognormal cumulative distribution function.

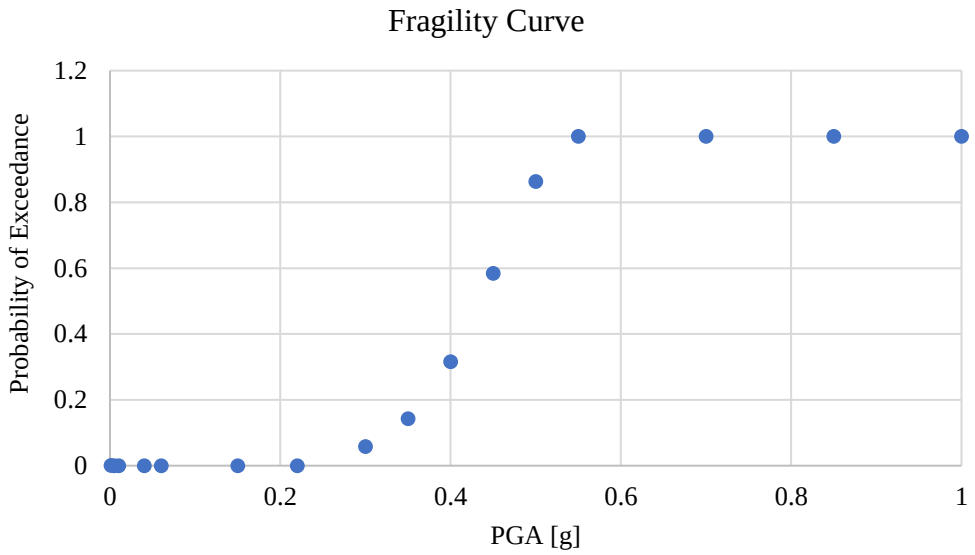

Figure 20 Fragility curve belongs to 1284 obtained by using lognormal cumulative distribution function.

MATLAB computer program was used to obtain smooth fragility curves of all structures. By providing the logarithmic distribution of the point representations obtained in the prepared MATLAB programming code, 6 different fragility curves were obtained. Figure 21 shows the fragility curves obtained for the selected buildings.

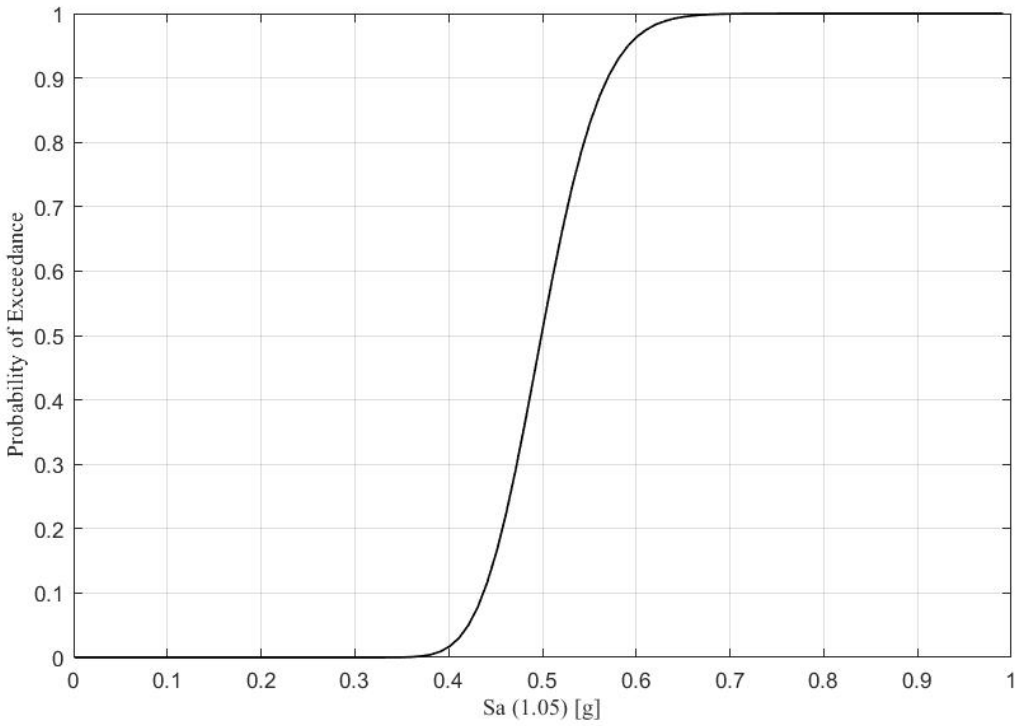

(a)

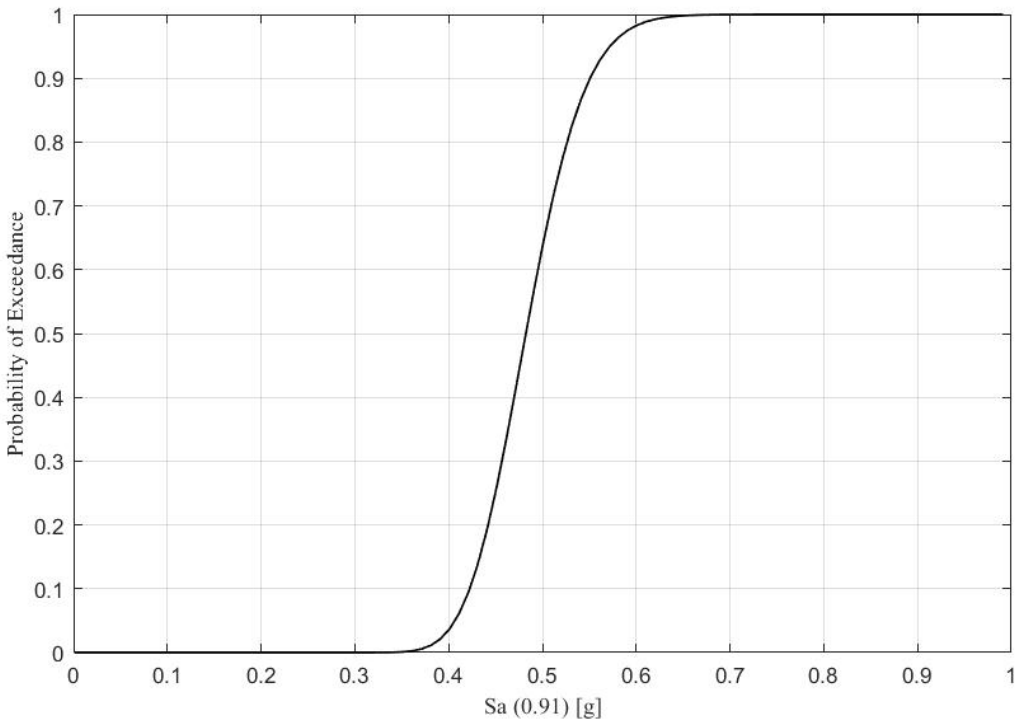
Probability of Exceedance
Sa (0.91) [g]
0
0.1
0.2
0.3
0.4
0.5
0.6
0.7
0.8
0.9
1

(b)

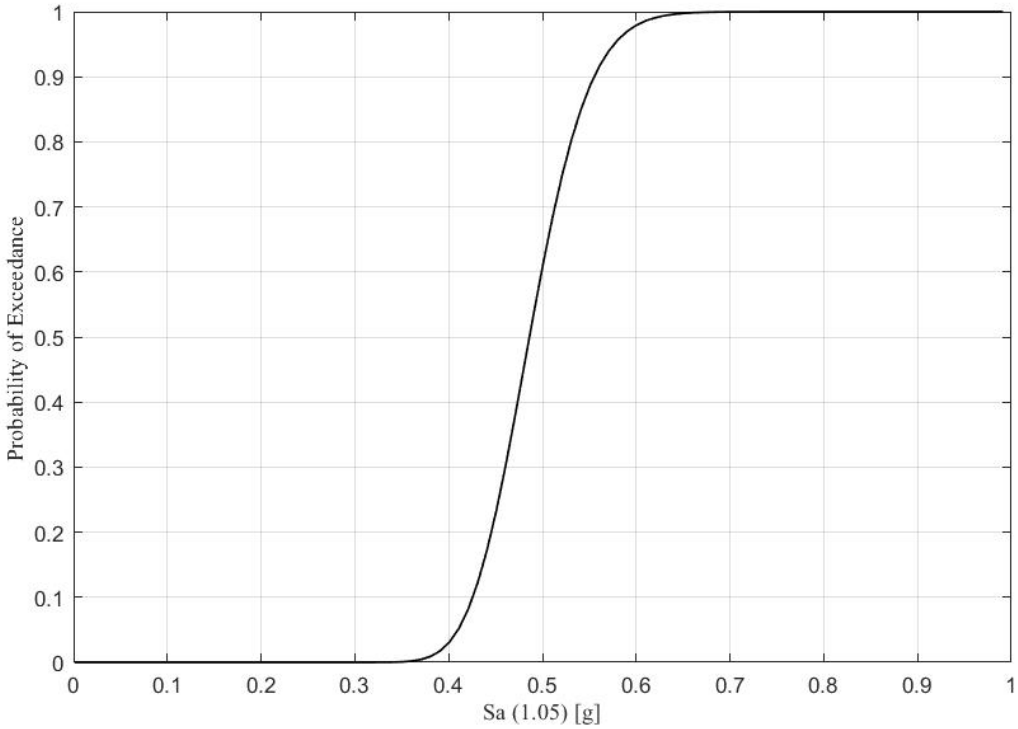
Probability of Exceedance
Sa (1.05) [g]
0
0.1
0.2
0.3
0.4
0.5
0.6
0.7
0.8
0.9
1

(c)

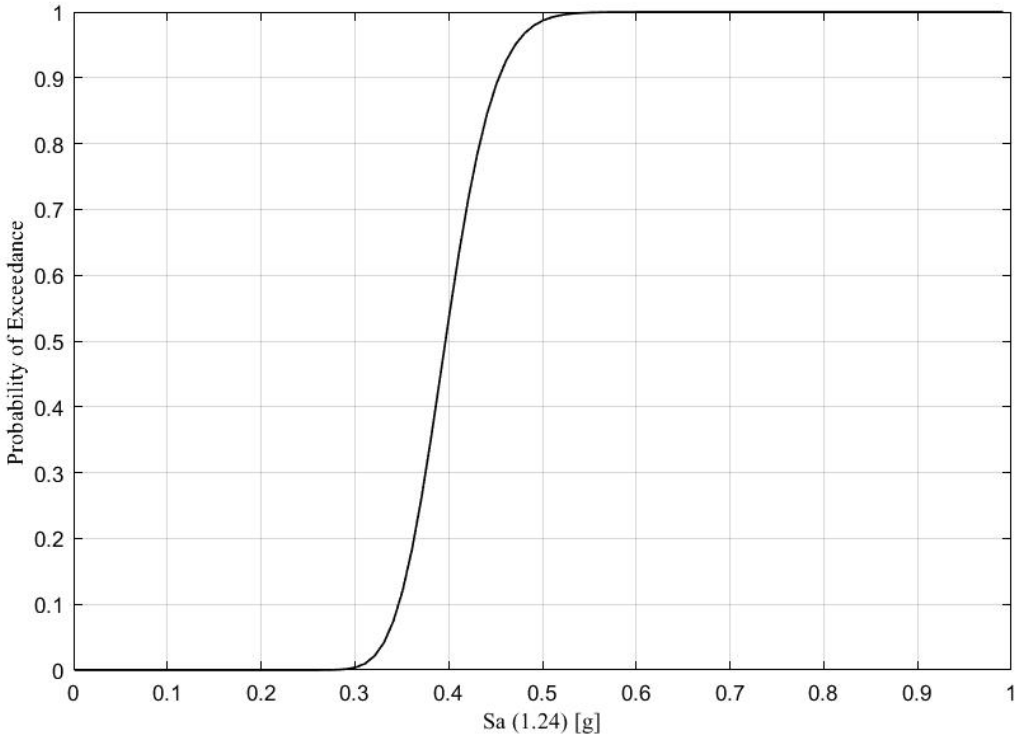
Probability of Exceedance
Sa (1.24) [g]
0
0.1
0.2
0.3
0.4
0.5
0.6
0.7
0.8
0.9
1

(d)

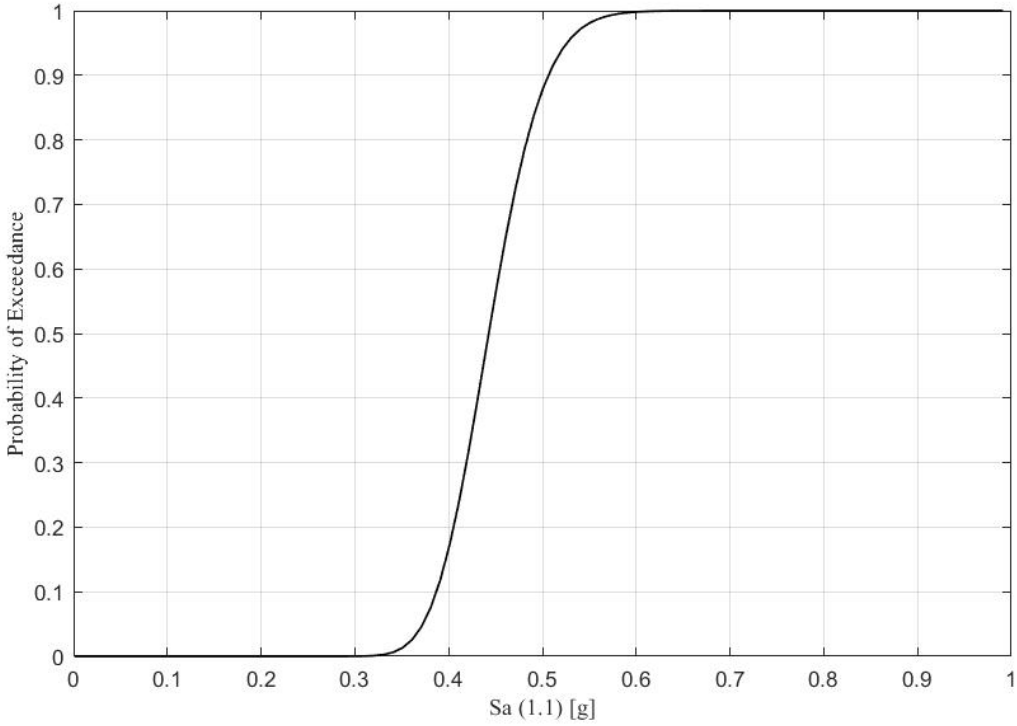
Probability of Exceedance
Sa (1.1) [g]
0
0.1
0.2
0.3
0.4
0.5
0.6
0.7
0.8
0.9
1

(e)

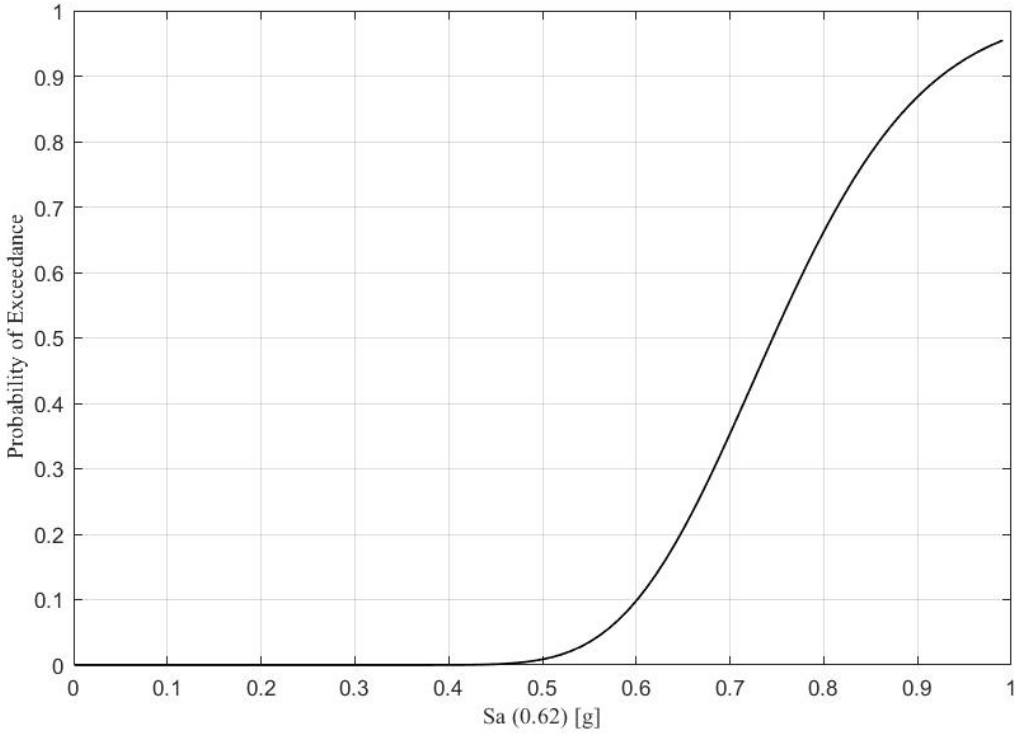

(f)

Figure 21 Fragility Curves for selected six building (a) 710-31 (b) 757-38 (c) 834-72 (d) 1113-197 (e) 1284-91 (f) 1427-87

When the fragility curves of the said 6 buildings are examined, it is seen that the probability of collapse of 1427 buildings is lower than other buildings. The two most important factors causing this are the ground condition and the natural vibration period of the structure. Again, considering the curves, it is seen that the building with the highest probability of failure is 1113, the biggest factor causing this situation is that this building has the highest natural vibration period. The fact that structures numbered 757, 834 and 710 have curves close to each other can be explained by the fact that both the natural vibration periods and Vs30 values of these structures are very close to each other. Tables 6 and 8 contain the features that are essential in the formation of the fragility curves of buildings, namely the features mentioned above. Figure 22 provides a representation of the fragility curve of 6 buildings in the same graph.

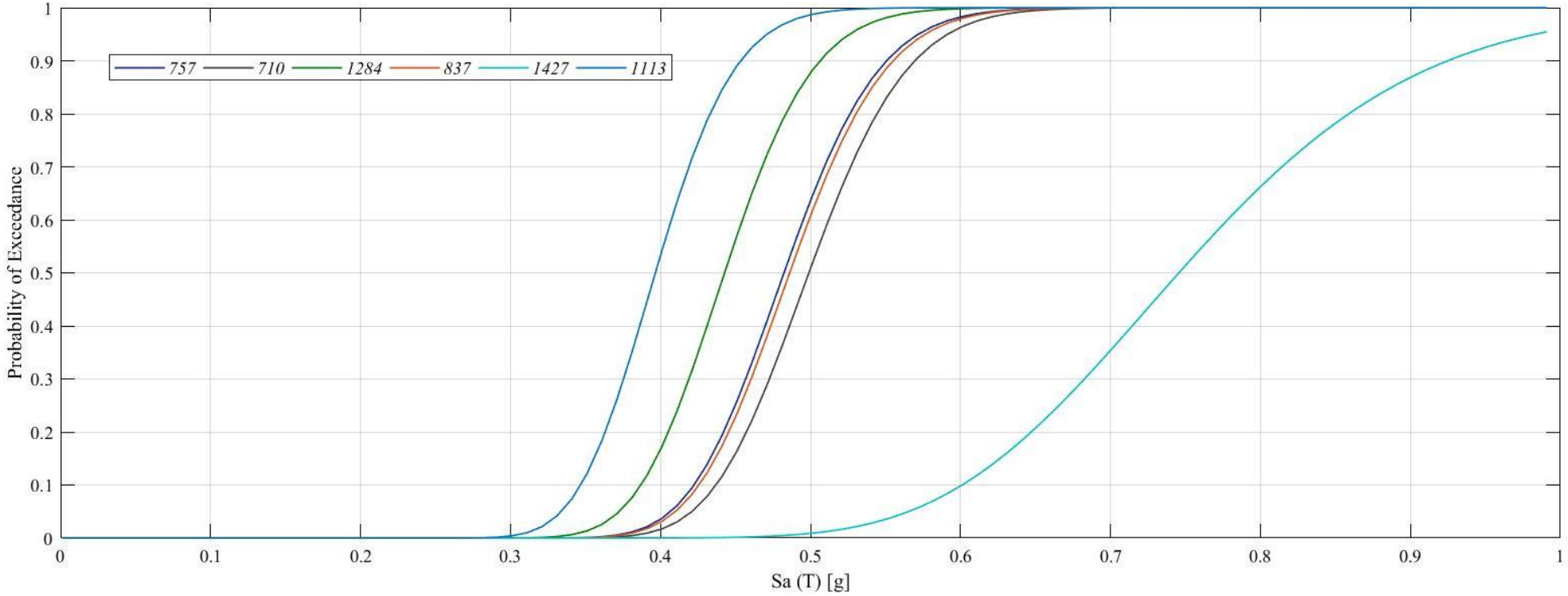

Figure 22 Fragility Curve

7. MDP

The MDP-based decision support method developed within the scope of this project works in 2 stages. When an earthquake occurs, the MDP achieves the maximum energized area before any maneuver is performed. In the second stage, physically action is taken in the field with the decision support mechanism. MDP updates the solution according to whether the actions are successful or failed.

The flow chart of the presented MDP generation method is shown in Figure 8. With the method, the details of which will be detailed in the next titles, in the system in which the calculations were not made in the first step, in the first case all the circuit breakers are open and the line states are not known. After that, a state s is taken from the set of iteratively uncalculated states, the set of lines $A^{-}(s)$ to which the restoration action can be applied for this state is calculated. Then, subsets of the set $A^{-}(s)$ satisfying the T1, T2, E1, and E2 constraints are calculated, and these subsets are added to the set A(s). If there is only an empty set a={ } in the set A(s), by loosening the limits of the FBPF analysis, the constraint check is repeated. In the next step, for each a∈A(s), the transition function defined in Equation (3) and Post(s,a) defined in Equation (4) are calculated. New states in the Post(s,a) set and that have not been encountered before during model creation are added to the uncomputed set of system states. This iterative process continues until all available system states are added to the model, that is, until the uncomputed state set is empty.

$$p(t|s,a) = \prod_{i\epsilon\, a} \begin{cases} P_f(s,i), & if\ t^i = D \\ 1 - P_f(s,i), & if\ t^i = E_k, k >= 0 \end{cases} \quad (3)$$

$$Post\,(s,a) = \{\, t \in S \mid p(t \mid s,a) > 0 \,\} \quad (4)$$

7.1 MDP Model

In this section, the proposed MDP-based restoration policy synthesis approach for the distribution system is described. Throughout the section, the number of buses, lines and DERs (including Batteries) of the distribution system considered are represented by N, L and T, respectively. K denotes the set of positive integers less than or equal to K value, that is, K = {1, ..., K}.

7.2 Model Setup

In the proposed MDP M = (S, A, p, c) model, each s∈S state represents the current state of all lines of the system. Thus, each state creates a snapshot of the distribution system. Status of a line:

1. Damaged (D)
2. Energizing has not been attempted yet, therefore the state of health is unknown (U)
3. It can be energized (E_i). Here the number i, $i \in \{0\} \cup \mathbb{L}$, indicates which source the line is connected to. When the source is the transmission network, the index is 0. In other cases, the index $i \in \mathbb{L}$ is the DER index that feeds the branch.

Thus, the state set S for MDP is defined as follows.

$$S = \{s_0, s_1, \ldots, s_F\}, \text{ where } s_i = [s_i^{\,1}, s_i^{\,2}, \ldots, s_i^{L}] \text{ and } s_i^{k} \in \{U, D\} \cup \{E_0, E_1, \ldots, E_T\} \quad (5)$$

The total number of states is limited from above by (3 + T)L according to Equation (8). However, most of these cases represent system configurations that are not possible, for example energized lines not connected to a source, a DER providing energy higher than its capacity, or the presence of ring structures is not possible. Such states are never added to the model. Thus, in practice, the size of S is much less than the given limit. Initially, all circuit breakers are assumed to be open. Thus, the initial state of the system is s0 = [U, U, ..., U].

Example 1: Figure 23 shows a system with 5 lines. Node-1 is connected to the transmission network and Node-6 is connected to a DER. The corresponding MDP status is s2 = [E0, E0, U, U, E1] indicating that the first and second lines are energized from the transmission network, the circuit breakers of the third and fourth lines are open and their condition is unknown. The fifth line receives energy from the DER.

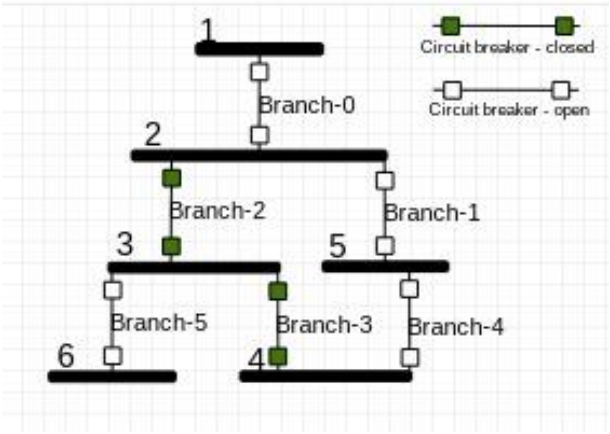

Figure 23 Example system with 5 lines

8. CASE STUDY

The resulting fragility curves were used as input for the Markov decision process (MDP) based decision support system designed for post-earthquake re-electrification. In order to show the effect of the fragility curves on the electrical paths selected in the system, the decision support system was run according to the exceedance probability values determined in the curves for 10 different g values, that is, for 10 different earthquake scenarios. These scenarios are shown in table 14.

Table 14 Probability of exceedance for six building with ten different g values

	Probability of exceedance for six building									
	g values									
Parcel number of buildings	**0.35**	**0.4**	**0.42**	**0.44**	**0.46**	**0.48**	**0.5**	**0.55**	**0.6**	**0.7**
710	0	0.01	0.05	0.12	0.28	0.35	0.52	0.85	0.97	1
757	0	0.02	0.08	0.24	0.4	0.5	0.62	0.89	0.99	1
834	0	0.02	0.08	0.22	0.37	0.48	0.64	0.91	0.99	1
1113	0.15	0.45	0.8	0.9	0.92	0.98	0.99	1	1	1
1284	0.05	0.18	0.35	0.58	0.67	0.8	0.87	0.99	1	1
1427	0	0	0	0	0	0	0	0.05	0.1	0.35
Other Busses	0	0	0	0	0	0	0.5	0.5	0.5	0.5

To illustrate the effects of fragility curves in the MDP system, an example of 30 buses from the Kadıköy electricity distribution system shown in Figure 5 was chosen. The selected exemplary system is shown in Figure 24.

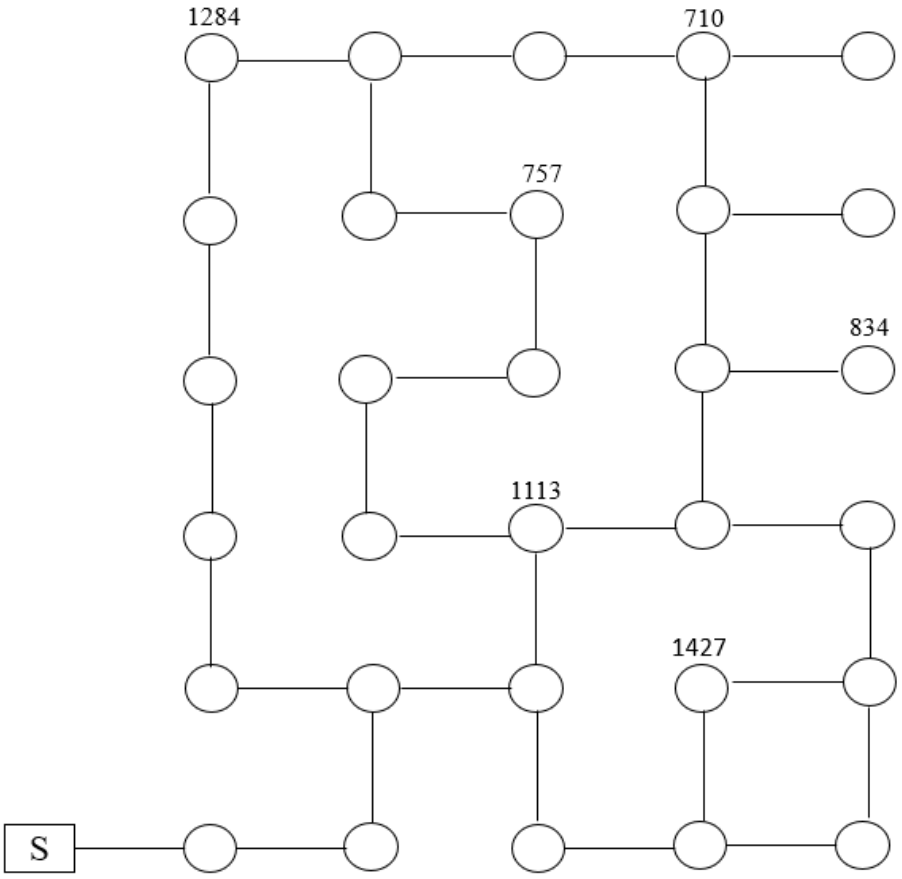

Figure 24 Sample system for MDP results

The system was run on this system with scenarios belong to table shown above. It was found that in the scenario, the transformers that were not affected by the 6 buildings not damaged up to 0.5 g, and in case of 0.5 g and higher g values, they were damaged with a 50% probability. Because when looking at past earthquakes and the behaviour of buildings in the pilot area, there is a 50 percent chance of collapse in earthquakes of 0.5 g or more.

According to Table 14, MDP system results were obtained by working on 3 different scenarios for 10 different earthquake situations. When the MDP system was run, 102 states for 0.35 g and 31 states for 0.7 g were created in scenario 2. That is, damaged bus detection at 0.7 g reduced the number of cases to one-third, even in a system with only 30 buses. At this point, reducing the number of states with the correct parameters provided by the fragility curves is very important for re-electrification, since the number of states

formed significantly affects both the operating speed of the MDP system and the optimal path selection.

To more specifically examine the variation between scenarios, the varying number of actions on the number of common situations are shown in Table 15.

Table 15 Action numbers for common states of all scenarios

	0.35	**0.4**	**0.42**	**0.44**	**0.46**	**0.48**	**0.5**	**0.55**	**0.6**	**0.7**
0.35	0	13	13	13	13	13	13	13	13	13
0.4	13	0	1	0	2	4	4	13	13	13
0.42	13	1	0	1	3	5	5	13	13	13
0.44	13	0	1	0	2	4	4	13	13	13
0.46	13	2	3	2	0	2	2	13	13	13
0.48	13	4	5	4	2	0	0	13	13	13
0.5	13	4	5	4	2	0	0	13	13	13
0.55	13	13	13	13	13	13	13	0	13	13
0.6	13	13	13	13	13	13	13	13	0	0
0.7	13	13	13	13	13	13	13	13	0	0

These results firstly show how much the use of curves changes the path chosen by the system, and without the right probabilities, the path to be used may provide post-earthquake re-electrification either very late or not at all. Another result that can be seen is how much each earthquake scenario affects the re-electrification path that can be effective. This study ensures that the most accurate possibilities for the post-earthquake usability of the electricity distribution systems are entered into the system, thus ensuring that electricity is supplied again as soon as possible, and thus the chaos after earthquake is managed in the shortest and most effective way.

9. CONCLUSIONS

In this study, fragility curves to be used as input to the Markov Decision Process (MDP) based decision support system developed for the rapid re-electrification of the regional electricity distribution system that was interrupted after the earthquake were obtained and the effects of these curves on the system were examined. Since Istanbul Kadıköy is one of the critical earthquake regions for our country, it was chosen as a pilot region and studies were carried out with real data about this region.

In order for the electricity distribution system to recover, first Autocad drawings showing the electricity distribution system of the pilot area were taken, these drawings were studied and the main sources providing the distribution were determined. In order for the re-electrification to be carried out in the shortest and most accurate way, the buildings that could prevent the electricity providers in the system from working and cause them to be damaged were determined. Damage to these buildings poses a danger to the electrical distribution systems in or around them, so their open addresses in the Autocad drawing and their locations on the map are marked in order to calculate the vulnerability of the buildings. A trip was organized to the pilot area, the points marked on the map were visited, and it was concretely checked whether the buildings would affect the electricity distribution systems. It was observed that the addresses of some buildings were missing, some buildings were demolished, and some buildings were in urban transformation. After the observations and studies conducted, 6 buildings that could damage the electricity distribution systems were identified.

A roadmap was created to create the fragility curves of selected buildings to provide input to the MDP system. According to this map, firstly the floor plans of the buildings were obtained, then the ground parameters of the buildings were determined according to the block and parcel numbers. Since the buildings were old, there were unreadable or missing parts in the floor plans. At this point, realistic assumptions were made by comparing the plans with each other and examining the regulations applied in the years they were made.

After the deficiencies in the floor plans were completed, the three-dimensional models of the buildings were prepared in the SAP2000 program. Since the use of real earthquake records while performing nonlinear time history analyses on buildings will give results closer to reality, modal analyses were first performed on the building models to determine the natural vibration periods of the buildings in order to obtain ground motion parameters.

The design spectrum of the buildings was drawn according to the Turkish Earthquake Code. The hazard spectra of the buildings were drawn using the Opensees program to determine the target spectrum. In order to select the earthquake records, the earthquake scenarios with the most effect were determined for the buildings according to the results of the deaggregation using the Opensees program. According to these parameters, earthquake records were downloaded from the PEER site. Among these records, 30 records were selected according to the conditional spectrum to be used in the analysis. These records were made ready for analysis by scaling them according to the uniform hazard spectrum of the buildings using the Seismomatch program.

To obtain the fragility curves of the buildings, roof displacements were calculated using 30 records in 2 axes for 5 different exceedance probability values, that is, 300 nonlinear time history analyses for a building. According to the exceedance probability values corresponding to the roof displacements obtained according to the results of the analysis, a ranking was made from the maximum to the minimum, and the collapse probability of the buildings was calculated using the lognormal cumulative distribution function. Later, these curves were used as inputs for the Markov Decision Process (MDP) based decision support system and were used as valuable parameters in finding the appropriate route for electricity for the Kadıköy region.

This study revealed how important the fragility curves are for the MDP-based decision support system used for re-electrification. Thanks to the studies, it was determined whether the electricity distribution systems were operational after the earthquake with results that are very close to reality obtained by using the specific fragility curves prepared for the real floor plans. Thanks to this study, for the MDP-based decision support system that can work online after the earthquake, studies were carried out with real scenarios on the basis of possible damage according to the earthquake magnitude, not archive information.

This study has been completed only for Kadıköy, and since the positive effect of this study on both material and moral losses after the earthquake is undeniable, further studies are planned to be conducted for other districts and even provinces.

This work can be done for large regions, for instance cities and even the whole country, by expanding the pilot area, increasing the selected buildings. For the shortest and most accurate re-electrification after the earthquake, the most important parameter is to

accurately predict and repair the damages that will occur after the earthquake. Therefore, carrying out this study in larger areas will be a very important and effective step to prevent loss of life and chaos that may occur after the earthquake.

10.REFERENCES

- R. C. Myrtle, S. F. Masri, R. L. Nigbor and J. P. Caffrey, Classification and prioritization of essential systems in hospitals under extreme event, Earthquake Spectra, 21(2005) 779–802.
- H. Sekiguchi and T. Iwata, Rupture process of the 1999 Kocaeli, Turkey, earthquake estimated from strong-motion waveforms, Bulletin of the Seismological Society of America, 92(2002) 300-311.
- M. Shinozuka, T.-C. Cheng, M. Feng and S.-T. Mau, Seismic performance analysis of electric power systems, Research Progress and Accomplishments 1997–1999, (1999) 61–69.
- A.-P. E. Cooperation, Earthquake disaster management of energy supply system of APEC member economies. Energy Commission, Ministry of Economic Affairs, (2002)
- M. Shinozuka, X. Dong, T. Chen and X. Jin, Seismic performance of electric transmission network under component failures, Earthquake Engineering & Structural Dynamics, 36(2007) 227-244.
- M. Shinozuka, S. Chang and T. Cheng, Advances in seismic performance evaluation of power networks, APEC Seminar on Earthquake Disaster Management of Energy Supply Systems, (2003).
- G. Parise, F. Ferranti and R. Colozza, Tentative criteria for the design and installation of electrical power systems subject to seismic hazard, IEEE Transactions on Industry Applications, 33(1997) 1342-1347.
- C. Nuti, A. Rasulo and I. Vanzi, Seismic safety evaluation of electric power supply at urban level, Earthquake Engineering & Structural Dynamics, 36(2007) 245-263.
- T. Adachi and B. R. Ellingwood, Serviceability of earthquake-damaged water systems: Effects of electrical power availability and power backup systems on system vulnerability, Reliability Engineering & System Safety, 93(2008) 78-88
- J.-M. Chevalier, Security of energy supply for the European Union, European Review of Energy Markets, 1(2006) 1-20.
- M. Shinozuka, S. E. Chang, T.-C. Cheng, M. Feng, T. D. O'rourke, M. A. Saadeghvaziri, et al., Resilience of Integrated Power and Water Systems,

Multidisciplinary Center for Earthquake Engineering Research (MCEER), US,2004.

- Y. S. Kim, Seismic Loss Assessment and Mitigation for Critical Urban Infrastructure Systems, University of Illinois at Urbana-Champaign, 2007.
- J. C. Araneda, H. Rudnick, S. Mocarquer and P. Miquel, Lessons from the 2010 Chilean earthquake and its impact on electricity supply, International Conference on Power System Technology, 2010, p.1-7.
- S. Wang, L. Hong and X. Chen, Vulnerability analysis of interdependent infrastructure systems: A methodological framework, Physica A: Statistical Mechanics and its applications, 391(2011) 3323-3335.
- Z. Cagnan and R. Davidson, Post-Earthquake Restoration Modeling Of Electric Power Systems, Proceedings of the 13th World Conference on Earthquake Engineering 2004, p.1-6.
- M. Ouyang and L. Duenas-Osorio, Multi-dimensional hurricane resilience assessment of electric power system, Structural Safety, 48(2014) 15-24.
- A. Arab, A. Khodaei, S. K. Khator, K. Ding, V. A. Emesih and Z. Han, Stochastic Pre-hurricane Restoration Planning for Electric Power Systems Infrastructure, IEEE Transactions on Smart Grid, 6(2015) 1046-1054.
- F. Qiu and P. Li, An Integrated Approach for Power System Restoration Planning, Proceedings of the IEEE, 105(2017) 1234-1252.
- Z. Zhao and B.-T. Ooi, Feasibility of fast restoration of power systems by micro-grids, IET Generation, Transmission & Distribution, 12(2018) 126-132.
- A. Golshani, W. Sun, Q. Zhou, Q. P. Zheng and J. Tong, Two-Stage Adaptive Restoration Decision Support System for a Self-Healing Power Grid, IEEE Transactions on Industrial Informatics, 13(2017) 2802-2812.
- N. Ganganath, J. V. Wang, X. Xu, C.-T. Cheng and K. T. Chi, Agglomerative Clustering Based Network Partitioning for Parallel Power System Restoration, IEEE Transactions on Industrial Informatics, 14(2017) 3325-3333.
- L. H. F. Neto, B. R. Pereira and G. R. da Costa, Smart Service Restoration of Electric Power Systems, IEEE Power and Energy Society General Meeting (PESGM), Boston, MA, 2016, p. 1-5.
- M. Ostermann, P. Hinkel, D. Raoofsheibani, W. H. Wellssow and C. Schneider, A minimum regret-based optimization approach for power system restoration in

EHV grids, IEEE Power & Energy Society General Meeting, Chicago, IL, USA, 2017, p. 1-5.

- C. Loh and Y. Huang, Seismic fragility analysis of Highway bridges, Monte Carlo Simulation, (2001) 505-511.
- MUNICIPALITY, T.I.M. and E.A.G.I. DIRECTORATE, Avs30 Distribution Map, 2009.
- T. Lin, C. B. Haselton and J. W. Baker, Conditional spectrum-based ground motion selection.Part I: Hazard consistency for risk-based assessments, Earthquake engineering & structural dynamics, 42(2013) 1847-1865.
- S. Akkar, M. A. Sandıkkaya and B. Ö. Ay, Compatible ground-motion prediction equations for damping scaling factors and vertical-to-horizontal spectral amplitude ratios for the broader Europe region, Bulletin of Earthquake Engineering, 12(2014) 517-547.
- Ö. Kale and S. Akkar, A ground-motion logic-tree scheme for regional seismic hazard studies, Earthquake Spectra, 33(2017) 837-856.
- D. M. Boore, J. P. Stewart, E. Seyhan and G. M. Atkinson, NGA-West2 equations for predicting PGA, PGV, and 5% damped PSA for shallow crustal earthquakes, Earthquake Spectra, 30(2014) 1057-1085.
- B. S.-J. Chiou and R. R. Youngs, Update of the Chiou and Youngs NGA model for the average horizontal component of peak ground motion and response spectra, Earthquake Spectra, 30(2014) 1117-1153.